Energy Conversion and Management 204 (2020) 112328

Contents lists available at ScienceDirect

Energy Conversion and Management

journal homepage: www.elsevier.com/locate/enconman

Proton exchange membrane fuel cells heat recovery opportunities for combined heating/cooling and power applications

Huy Quoc Nguyen, Bahman Shabani*

Mechanical & Automotive Engineering, School of Engineering, RMIT University, Bundoora, Victoria 3083, Australia

ARTICLE INFO

Keywords:
PEM fuel cell
Thermal management
Fuel cell heat recovery
Low-grade heat recovery
CHP
CCHP

ABSTRACT

The present paper provides a comprehensive review of heat recovery opportunities for proton exchange membrane fuel cells. A significant amount of heat is generated by these fuel cells while operating that is equivalent to ~45 to 60% of the total energy content of hydrogen entering the cells. The generated heat must be removed effectively from the stack by using a properly-designed cooling system in order to prolong its lifetime and maintain its performance. Applying proper thermal management strategies and capturing opportunities for fuel cell heat recovery can add significant values to a fuel cell system in terms of size, costs, and its overall energy efficiency. The heat generated by proton exchange membrane fuel cells can be captured and used for a range of combined heating/cooling and power applications: i.e. combined heat and power, combined cooling and power, or combined cooling heat and power solutions. The heat generated by a fuel cell stack also provides opportunities for its integration with organic Rankine cycles, thermoelectric generators, and thermally regenerative electrochemical cycles for power cogeneration applications. Furthermore, the heat recovered from a fuel cell can be used for self-servicing the system such as enhancing the hydrogen discharge rate of metal hydride canisters (supplying hydrogen to the stack) or preheating inlet air and hydrogen to improve performance of the fuel cell. The present paper also helps identify the research gaps in this area and provides direction on future studies on thermal management and integrated heat recovery solutions for proton exchange membrane fuel cells.

1. Introduction

Shifting away from fossil fuels and moving towards renewable energy resources such as wind and solar and applying energy efficiency measures are receiving increasing attention globally. This is in fact a response to soaring price of conventional fossil fuels and increasing level of greenhouse gas (GHG) emission [1,2]. However, the key challenge facing the widespread utilisation of renewables is their intermittent nature that makes them incapable of providing a continuous and reliable supply of energy without being accompanied by suitable energy storage solutions [3].

Hydrogen has emerged as a promising energy carrier for a range of stationary [4,5] and mobile/transportation applications [6]. Using hydrogen in this capacity is becoming more viable economically these days specially for large-scale and/or long-term energy storage applications [7,8]. Moreover, having higher volumetric energy density compared to other storage technologies (e.g. over 50 times higher than compressed air and 200 times better than pumped hydro storage [9]) enables hydrogen to offer a greater degree of practicality. Supporting renewables through a reliable energy storage solution can in turn encourage their penetration that would significantly help reduce GHG emissions [9–11]. Even in hydrogen systems with original fossil fuel feed, the advantage of GHG reduction can be observed [12]. For instance, cogeneration systems based on hydrogen obtained through steam reforming of natural gas, to power fuel cells, can still reduce carbon dioxide (CO_2) and nitrogen oxides (NO_x) emissions by up to 49% and 91%, respectively, compared with when traditional combustion technologies are used [13]. Zero-emission can be achieved if hydrogen is generated completely using renewable energy sources such as solar and wind (e.g. through water electrolysis) [14].

In a hydrogen fuel cell, the chemical energy of hydrogen is converted directly to DC electricity at a relatively high electrical energy efficiency of up to ~55%, based on the high heating value (HHV) of hydrogen [3]. There are several types of fuel cell technologies mainly categorised based on the membranes used and the mobile ions involved, including polymer electrolyte membrane (PEM), solid oxide (SO), alkaline, direct methanol (DM), phosphoric acid (PC), and molten carbonate (MC) fuel cells. Among these different types of fuel cells, PEM fuel cells (PEMFC) have been widely recognised as a promising technology for a range of stationary, transportation, auxiliary, portable, and

* Corresponding author.
E-mail address: bahman.shabani@rmit.edu.au (B. Shabani).

https://doi.org/10.1016/j.enconman.2019.112328
Received 2 October 2019; Received in revised form 19 November 2019; Accepted 21 November 2019
Available online 29 November 2019

Nomenclature

Abbreviations

CCHP	combined cooling, heat and power
CCP	combined cooling and power
CHP	combined heat and power
CO	carbon monoxide
CO_2	carbon dioxide
COP	coefficient of performance
DM	direct methanol
FC	fuel cell
GHG	greenhouse gas
HHV	high heating value
HT	high-temperature
LT	low-temperature
LHV	low heating value
LiBr	lithium bromide
MH	metal hydride
MC	molten carbonate
NH_3	ammonia
NO_x	oxides of nitrogen
ORC	organic Rankine cycle
PEM	polymer electrolyte membrane
PC	phosphoric acid
PV	photovoltaic
PV/T	photovoltaic thermal
SO	solid oxide
TEC	thermoelectric cooler
TEG	thermoelectric generator
TREC	thermally regenerative electrochemical cycle
ZT	figure of merit

Symbol

A	area, m^2
ΔG	Gibbs free energy
F	Faraday constant
ΔH	enthalpy change, J/mol
i	current density, A/cm^2
I	current, A
k	thermal conductivity, W/mK
$\dot{m}$	mass flow rate, kg/s
P	pressure, N/m^2
Q	heat, J
$\dot{Q}$	heat rate, W
t	time, sec
T	temperature, K
S	Seebeck coefficient, V/K
ΔS	entropy change, J/molK

Greek symbol

A	charge transfer coefficient
η	energy efficiency
σ	electrical conductivity, S/m
φ	temperature coefficient
ρ	density, kg/m^3

Subscripts and superscripts

act	activation
C	cold
con	concentration
cell	single cell
d	desorption
EL	electrolyser
elec	electricity
eq	equilibrium
FC	fuel cell
H	hot
L	limitation
ohm	ohmic
PV	photovoltaic
Re	heat recovery
s	solid
SPV	solar PV
th	thermal
WT	wind turbine

mobile power supply applications [15]. This is because PEMFCs offer many advantages compared to conventional energy conversion technologies such as rapid start-up (less than 30 s), low operating temperature (i.e. 60–80 °C for low-temperature PEMFC known as LT-PEMFC [16–19] and 120–200 °C for high-temperature PEMFC known as HT-PEMFC) [20,21]), high electrical energy efficiency (up to 55% based on HHV of hydrogen) [3,22,23], and quick response to highly dynamic loads [19,24].

It is important to note that a considerable amount of heat, equivalent to ~45 to 60% of the total energy content of hydrogen, is also generated as the result of PEMFC operation [25–27]. The operating temperature of a LT-PEMFC must be maintained in the range of 60–80 °C to avoid issues associated with overheating [16,25] or flooding of the membrane that can occur at low operating temperature (i.e. particularly in the absence of proper water management solutions) [28,29]. The generated heat must be removed effectively from the fuel cell by using a properly-designed cooling means in order to prolong the lifetime and performance of the PEMFC. By taking into account the significant amount of heat generation when operating a PEMFC, heat recovery from the PEMFC systems (i.e. for supplying both heat and power) becomes an attractive idea in order to improve the overall energy efficiency of the fuel cells and reduce their operating costs while offering a new opportunity to further reduce GHG emissions generated by fossil fuels normally used for on-site thermal applications [14].

The heat recovered from PEMFCs can be used for low-temperature heating applications such as space heating and domestic hot water supply that need low-grade heat [24,30–36]. Many studies showed that by capturing the fuel cell heat to supply both hot water and electricity to residential households, the overall energy efficiency of a PEMFC in combined heat and power (CHP) mode can increase to ~60 to 90% [3,12,33,37], which is much higher than when the fuel cell is used for supplying electricity only. The heat generated by the fuel cell stacks can also be captured to drive sorption cooling cycles for combined cooling and power (CCP) or combined cooling, heating and power supply (CCHP) purposes [38]; or be integrated with organic Rankine cycles (ORCs) [39,40], thermoelectric generators (TEGs) [18,41] and thermally regenerative electrochemical cycles (TRECs) for power cogeneration applications. Furthermore, the heat recovered from PEMFC stacks has also been used for other purposes such as enhancing the hydrogen discharge rate of metal hydride (MH) canisters [42–44] or preheating inlet air [24] and hydrogen especially in cold climate conditions [45].

In general, the notion of waste heat recovery has been widely applied in a range of energy conversion systems (e.g. boiler, gas turbines, diesel engines, industrial process, etc.) for many decades [46–48]. Meanwhile, investigating the potential of waste heat utilisation from fuel cell systems, to increase their overall energy conversion efficiency, has received significant attention by scientists, particularly in recent years [37,49]. Despite a number of publications related to fuel cell-based CHP, CCHP, and CCP systems, limited comprehensive and systematic reviews with specific focus on fuel cell heat recovery and applications are available in the literature. The paper published by Ellamla et al. [12] is one of the most recent reviews on this topic that is limited to fuel cells-based CHP systems for residential applications by focusing on technical, environmental, and economic characteristics of such systems. Elmer et al. [11] have also conducted a similar review in which they emphasised on maintenance, durability, cost, and optimisation considerations of fuel cell CHP and CCHP systems operating in the domestic built environment. Milcarek et al. [50] focused on discussing methods of assessing the fuel cell micro CHP for residential applications via mathematical models. Most of these review papers considered all types of fuel cells (i.e. PEMFC and SOFC) and looked at their heating and cooling (alongside with power) generation for residential sector applications only. Most recently, in 2018, another limited review was published by Özgür and Yakaryılmaz [51]. In this paper, they reviewed the PEMFC and PEMFC-CHP systems using, exergy analysis, by focusing on key operating parameters, including temperature, pressure, stoichiometry, and membrane thickness.

The comprehensive review of the literature conducted to support this work, indicated that the previous reviews are mainly focused on micro CHP-based fuel cells using hydrocarbons reforming technologies for residential applications. However, as discussed in this section, the applications for the heat recovered from PEMFCs can go beyond micro CHP systems. This heat can be utilised for a wide range of other purposes, such as CHP, CCHP, power cogeneration, and preheating applications, to help improve the overall energy efficiency and performance of different PEMFC-based energy systems. Therefore, the present work is trying to address this gap by specifically focusing on PEMFC heat recovery in above-mentioned applications. The discussion starts with a brief review of thermal management arrangement practiced for PEMFCs in order to understand how heat is generated and recovered in PEMFCs for use in different applications. This study is then followed by a critical specific review of PEMFC-based CHP, CCP, and CCHP systems and summarising the key findings reported in the literature. Finally, this work is supported by an extensive discussion to shed light on merits of such combined heating/cooling/other applications from the points of view of energy and exergy efficiencies.

2. Fuel cell thermal management and heat recovery opportunities

Heat recovery can help add value to fuel cell systems by improving their overall energy efficiency their economic performance. As already discussed in Section 1, to satisfy the technical needs of PEMFCs, their operating temperature must be maintained within desirable ranges (i.e. 60–80 °C for LT-PEMFC and 120–200 °C for HT-PEMFC). Furthermore, temperature distribution within the stack should be kept uniform to avoid local hot spots, which particularly accelerate the mechanical degradation of their membranes [23,52]. For designing a PEMFC-based heat recovery system (i.e. for CHP applications), the type of fuel cell, its cooling system arrangement, and the thermal and power applications that the system is used for should be taken into consideration. It is noteworthy that PEMFCs' thermal management techniques are briefly reviewed in this section to provide a better understanding of opportunities for heat recovery in PEMFCs and the applications. The comprehensive review of PEMFC thermal management can be found in the review papers [16,17,52].

2.1. Fuel cell heat generation

Heat generation in PEMFCs is due to entropic heat of reactions (~35% of total heat) and a range of irreversibility (~65% of total heat) linked to hydrogen gas crossover, the activation of the electrochemical reactions, ohmic resistances against the flow of protons (i.e. in membranes) and electrons (i.e. at both cell and stack levels), and mass transport of hydrogen to the anode [16,17,52,53]. The amount of heat generated in a fuel cell stack is determined by comparing the voltage of a single cell with output voltage of a 100% efficient fuel cell. The value of maximum voltage is 1.48 V based on HHV of hydrogen (i.e. if the water product is assumed to be in liquid form), and 1.25 V based on LHV (i.e. if the water leaves the stack in vapour form) [15,54]. It is noteworthy that in practice, part of heat generated by the fuel cell is used internally to evaporate the water product within the cell during operation. Therefore, the total generated heat (Eq. (1)) is calculated based on HHV, while the cooling load of the stack (Eq. (2)) is based on LHV by considering the amount of heat demanded internally to evaporate mainly the water produced during the operation [24,42].

$$\dot{Q}_{FC-gen} = \mathrm{N.\ i.\ A}_{cell}(1.48 - V_{cell}) \tag{1}$$

$$\dot{Q}_{FC-cooling} = \mathrm{N.\ i.\ A}_{cell}(1.25 - V_{cell}) \tag{2}$$

In these equations, i is current density, (A/cm^2); A_{cell} is the active area of a single cell (cm^2); N is the number of cells in the stack; and V_{cell} is the actual voltage of a single cell (V).

Due to overpotentials including internal current, activation overpotential (ΔV_{act}), ohmic overpotential (ΔV_{ohm}), and concentration (mass transport) (ΔV_{con}), the cell voltage drops from its level at open circuit condition (E_{Nernst}), while delivering electrical power to a load. Thus, the actual voltage of a single cell (V_{cell})is determined using Eqs. (3) and (4) [14,25].

$$V_{cell} = \mathrm{E}_{Nernst} - \Delta V_{act} - \Delta V_{ohm} - \Delta V_{con} \tag{3}$$

$$V_{cell} = \left[E_0 + \frac{RT}{2F} ln\left(\frac{P_{H_2}.\ P_{O_2}}{P_{H_2O}}\right)\right] - \frac{RT}{2\alpha F} ln\left(\frac{i}{i_0}\right) - i.\ r - \alpha_1 i^k \ln\left(1 - \frac{i}{i_L}\right) \tag{4}$$

where E_0 is the electromotive force (EMF); R is universal gas constants (8.314 kJ/mol.K); T is the stack temperature (K); F is the Faraday's constant (96485 C/mol); P_{H_2}, $P_{O_2}$and P_{H_2O} are the partial pressures of hydrogen, oxygen and water respectively (N/m^2); α is charge transfer coefficient; r is the area-specific resistance (Ω/cm^2); $\alpha_1$is the amplification constant; and i_L is the limiting current density.

As indicated in above-mentioned equations, the heat generated in the fuel cell increases by increasing the current density. Fig. 1 is an example showing the actual voltage, power output, and heat generation density in a typical single PEMFC at various current densities. It is important that the values on this graph (i.e. Fig. 1) can vary in different PEMFCs and/or different operating and fuel cell conditions.

The amount of heat generated in a PEMFC usually accounts for up to about 60% of the total reacted hydrogen energy content and part of this heat (around 25–35%) is removed out of the fuel cell stack by extra

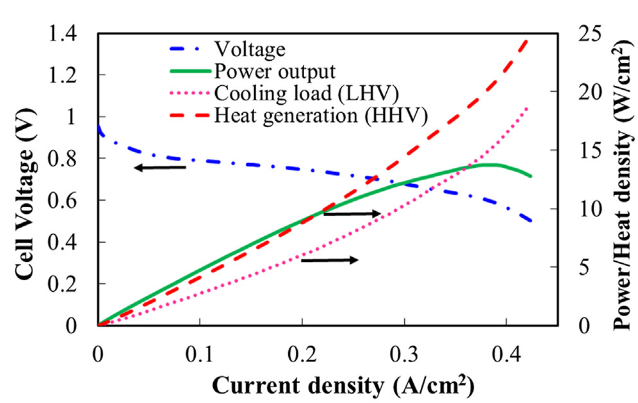

Fig. 1. Typical heat generation behaviour of a PEMFC at different current densities [16].

reactants as well as the latent heat of water vaporisation (i.e. the product of hydrogen and oxygen reaction) [14]. The remaining heat, known as cooling load (Eq. (2)), is rejected through a purposely-designed cooling system with a small portion lost from the body of the fuel cell (e.g. through natural convection). Fig. 2 shows a typical Sankey diagram for the flow of hydrogen energy throughout a PEMFC experimentally obtained by Shabani and Andrews, after applying thermal insulation over the body of the fuel cell [33].

2.2. Thermal management strategies

The size of a fuel cell is an important parameter to consider before choosing a right cooling strategy/technique for it. Cooling techniques applied for PEMFC thermal management are summarised in the Table 1. While simple cooling methods such as using heat spreaders, heat pipes, and cathode air supply are normally employed for small size PEMFCs (i.e. < 2 kW), the liquid cooling strategies (i.e. using water, glycol and nanofluids as coolants) is widely used in high power fuel cell stacks (i.e. > 5 kW) [17,26]. The selection of cooling systems for the medium cell stacks, i.e. between 2 kW and 5 kW, is though done by considering a range of above-mentioned options according to the design and by considering the operating condition of the stack. The application of heat recovery has significant impacts on the decision of whether air or liquid coolant is used for the cooling system. For example, heat recovery from the airflow in air-cooled fuel cells can be a preferred option for preheating the inlet air in an extreme cold environment [24] or thermal coupling with metal hydride [55]. Meanwhile, liquid-cooled fuel cells are usually favourable for domestic CHP applications (i.e. hot water and space heating) due to the larger thermal capacity and more favourable heat transfer properties of liquid coolants (e.g. water) compared to air [52].

2.2.1. Edge cooling

Edge cooling is usually a passive cooling technique that uses spreaders to cool down fuel cells through extended surfaced. High thermal conductivity materials are placed within the cooling plates of the fuel cell to take heat from central regions of the active area and transfer it to the edges of the cells.

This can be done using different means: One of the common approaches is using heat spreaders in which low-density graphite-based material (i.e. expanded graphite and pyrolytic graphite) with 600–1000 W/mK of thermal conductivity are employed [58,59]. By employing high performance heat spreaders the mass of the fuel cell stacks can be reduced [59,60]. However, this technique usually offers less flexibility in controlling the cooling conditions and the temperature of the stack, and hence it is mostly used in low-power fuel cell stacks. Heat recovered using this type of cooling system can also be fed into thermoelectric generator [18,61,62]. The electricity generated can then be used for running the referrals of the system. This idea will be further discussed later in this paper.

Another technique is using heat pipes integrated into the bipolar plates or dedicated separate cooling plates of the fuel cell stack, as shown in Fig. 3. Due to their high effective thermal conductivity (2100–50,000 W/mK [63–65]), with a small cross-section area and without requirement for additional power input (e.g. fans and pumps), heat pipes can remove a large amount of heat [16,66]. Using heat pipes for cooling PEMFC stacks has proven to be an effective and a feasible thermal management strategy for long-term operation [67]. For example, Burke et al. [66] experimentally investigated the thermal management of a PEMFC stack under NASA exploration programs using planar heat pipes. They found that very high thermal conductivity of heat pipes (up to more than 20,000 W/mK) made it feasible to be applied for large PEMFC stacks. Oro and Bazzo [68] proposed thin flat heat pipes to remove a heat flux of 0.2 W/cm^2 from PEM fuel cell. The results showed that the flat heat pipes meet the required heat dissipation capacity and operating temperature for the fuel cell. Several types of heat pipes including micro/mini (< 10 W), loop (10–100 W heat removal capacity), and pulsating (100–1000 W capacity) heat pipes have been applied for PEMFC cooling applications by Clement and Wang [69] and Vasiliev [70,71]. Using heat pipes for cooling of small-size PEMFCs eliminates the need for ancillary cooling components (i.e. pumps, fans and pipe connections), hence helps reduce the weight and volume of the system while improving its overall energy efficiency.

2.2.2. Air cooling

For small-size open-cathode LT-PEMFC stacks (i.e. 100–1000 W), cooling can be performed by increasing the cathode air flow rate. This method of cooling has also been practiced in HT-PEMFCs [21,72]. Forced cooling using the cathode air flow supplies extra oxygen for electrochemical reactions that can be desirable in some operating modes and conditions [73]. However, this fact should be considered that the higher stoichiometric of air supply (e.g. 8 or above [44]) can contribute to drying out the membrane that results in significant degradation of stack's performance and impacts its lifetime [74]. Another disadvantage of this cooling method is that the temperature cannot be controlled precisely because the cooling performance is always

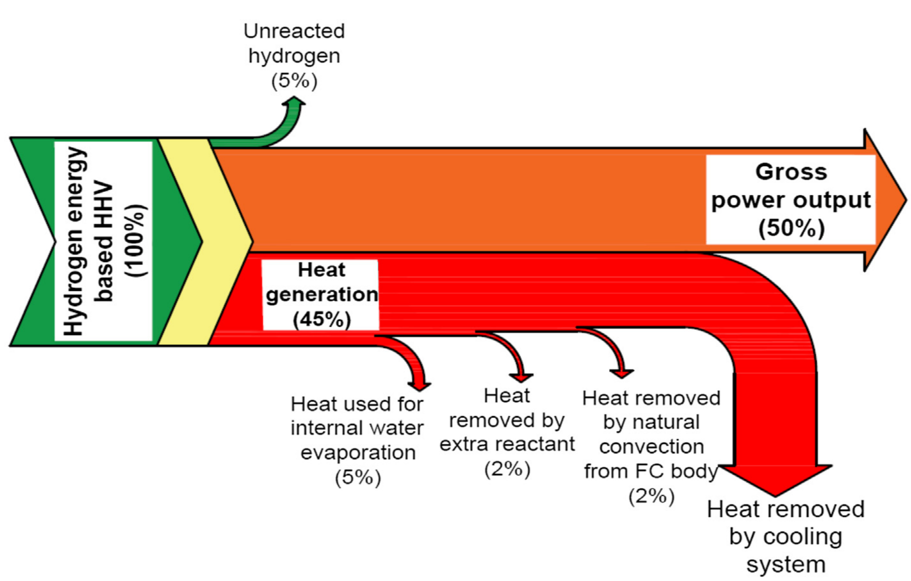

Fig. 2. A typical energy flow diagram in a PEMFC [33].

Table 1
Cooling techniques and heat recovery applications for PEMFCs [16,56,57].

Cooling techniques	Techniques/Materials	Advantages	Disadvantages/Challenges	Heat recovery applications
Edge cooling	Using highly thermal conductive materials such as copper or heat pipes as heat spreaders	- Simple system - Low parasitic power - Very high thermal conductivity - No coolant circulation systems	- Limited heat transfer length (i.e. copper) - The design and fabrication of heat pipes integrated into PEMFC stacks	- Preheating reactants - Metal hydride thermal management - Integration with TEG
Air cooling	- Using excessive cathode air flow for 100–1000 W stacks - Using separate air flow channels for cooling	- Simple system - Low parasitic power - Potential integration for fuel cell oxygen supply	- Drying membrane - Precise temperature control - Trade-off between performance and parasitic power.	- CHP (i.e. space heating) - Preheating reactants - Metal hydride thermal management - Integration with TEG
Liquid cooling	Cooling channels integrated into bipolar plates using DI water or anti-freezing coolants	- Large cooling capability - Flexible control of cooling capability - Efficient cooling	- High parasitic power - Large radiator size and packaging implications - Coolant degradation	- CHP - CCP/CCHP - Power generations (i.e. integration with ORCs or TRECs) - Preheating and thermal management
Phase change cooling	Evaporative or boiling cooling using latent heat absorption	- Simultaneous cooling - Simple system - Elimination of coolant pump	- Evaporative rate control - Development the suitable working media - Instability of two-phase flow	- Preheating reactants - Metal hydride thermal management - Integration with TEG - Space heating

influenced by the ambient temperature and humidity [52].

The fuel cell performance degradation problems caused by excessive cathode air flow (i.e. drying out the membrane) can be resolved by separating the reactant air supply and the air stream used for cooling purpose [15]. By doing so, such an air-cooling technique can also be practiced in close-cathode PEMFCs. While inlet reactant air is controlled for optimal chemical reactions, air coolant flow is applied through separate channels on either bipolar plates or through purposely-design cooling plates, by using fans or blowers. Sohn et al. [75] fabricated and tested a 500 W PEMFC with forced air-cooling from fans to evaluate the design performance and determine optimal operating conditions. The results showed that the air temperature and relative humidity have significant impacts on the performance of the fuel cell stack. The parasitic load associated with the fan was determined to be 2% of the overall power output. Integrating cooling plates into the fuel cell stack allows for having more control on cooling and thus the temperature gradient across the cells can be reduced by applying a proper control on the cooling condition [76]. Matian et al. [77] numerically and experimentally investigated three different cooling plate designs for an air-cooled PEMFC stack. It was found that the cooling plate design, which has larger cooling channels, shows more uniform temperature distribution. Recently, using separate air cooling plates has been also practiced in some commercially-available stacks, in range from 100 W to 5000 W, such as Ballard's FCgen®-1020ACS [78] and Horizon open-cathode H-Series [79] (Fig. 4).

For heat recovery applications, because of low thermal conductivity and specific heat capacity of air, heat from cooling air flow is normally used for specifically low-grade thermal applications such as preheating reactants, space heating, or thermal management of metal hydride hydrogen storage canisters [24,44].

2.2.3. Liquid cooling

This method is usually used for large-size fuel cell stacks (i.e. > 5 kW); however, smaller size fuel cells can still be equipped with liquid cooling systems (i.e. FCvelocity–9SSL [78], PowerCell S2 [80] and Gendrive GD3 [81]). The high power generation means that more heat is generated by the stack [15] that air is not usually effective in removing it all, particularly from a limited surface area. Liquid coolants (i.e. water, water-ethylene glycol, and nanofluids) have significantly higher heat removal capacity than air, mainly due to higher thermal conductivity and convection factor [82,83]. Schematic diagram of a typical liquid-cooled PEMFC cooling system is illustrated in Fig. 5.

A key benefit of the liquid cooling strategy is the flexibility for utilisation of the system in a broader range of heat recovery applications in comparison with when other cooling methods are used (e.g. air cooling) are used. This includes:

- Hot water supply [84,85];
- Space heating [86];
- Driving thermodynamic cycles (e.g. an organic Rankine cycle [19,87] and sorption cooling cycles [88,89]); and
- Operating thermoelectric cells [41,90].

The heat recovery opportunities from the coolant loops for such applications will be further discussed in the following sections.

There are also some challenges associated with liquid cooling such as current leakage particularly to coolants with high electrical conductivity [91–93], coolants freezing in sub-freezing environment, and the overall complexity of the system compare to other cooling arrangements [24]. To prevent the current leak issues, solutions such as placing a de-ionisation filter in the cooling circuit and using ion-exchange resin and antioxidant additives are employed [26]. For operating in the sub-freezing conditions antifreeze coolants (e.g. mixture of water and ethylene glycol) are used; however, this should be noted that usually these anti-freezing agents reduce the thermal conductivity of the coolants that affects their heat removal capacity [93]. As detailed in

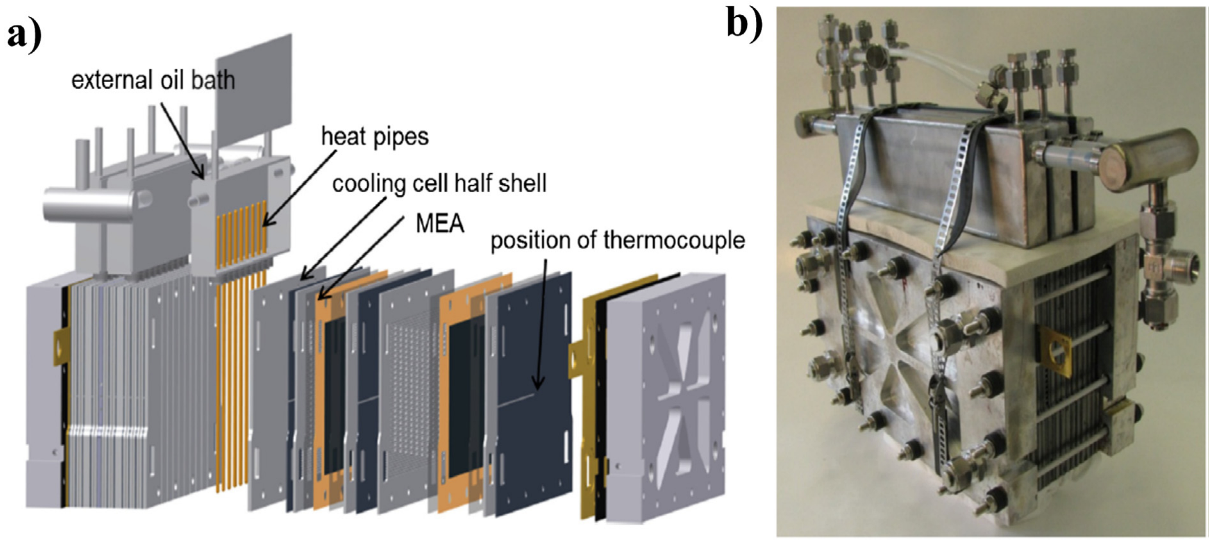

Fig. 3. PEM fuel cell thermal management using heat pipe. a) Structure of cell with integrated heat pipes; b) a 10-cell stack with 200 cm^2 active MEA area [63].

Fig. 5, multiple components used in liquid-cooled systems (i.e. pump, pipes, de-ionising unit, and heat exchanger) that adds to the size and mass of the system while increasing its maintenance cost. The size of the system may not be a critical matter in stationary applications; however, in vehicle application for which liquid cooling is the most feasible solution, space limitation is always a challenge. Particularly, in PEMFCs due to limited temperature difference between the stack (i.e. 60–80 °C) and ambient (e.g. up to 50 °C in hot climate), the driving force for heat transfer is weak suggesting the requirement for relatively large size heat exchangers (radiators) in the system [26,94].

2.2.4. Phase change cooling

The phase change cooling techniques utilise the latent heat of the coolant to absorb and transfer the heat generated by fuel cell stack to outside. Due to high latent heat, this method requires a much lower coolant flow rate than liquid cooling or air cooling. In addition, the coolant pumps can be eliminated because phase change coolant can be circulated through hydrophilic wicking, pressure difference or density difference [16,95]. Evaporative cooling and cooling through boiling are two basic approaches of phase change cooling applied in PEMFC thermal management.

In evaporative cooling, the water is typically used because the boiling temperature of the coolant is higher than operating temperature of the PEMFC stack [16,95–97]. The heat generated in the cells is removed by phase transient of the water (from liquid to vapour) while maintaining their temperature constant. This cooling technique has the advantage of humidifying membrane in the cell while eliminating removing the need for both external humidifiers and separate cooling plates within the stack [98,99]. A challenge of this technique is supplying the water into the cells at a certain rate to make sure the evaporation to be continued. Several methods was applied for water evaporative cooling including direct introduction of the liquid water into the reactant gas channels [100], integrating wicking material with bipolar plates [101], and using porous water transport bipolar plate [102].

Cooling through boiling has the benefit of offering a very high cooling capability. To make it applicable, the boiling temperature of the coolant has to be lower than the operating temperature of PEMFC stacks that should be considering for selecting a suitable coolant. Garrity et al. [103] developed cooling plates using HFE-7100 coolant to investigate the impacts of the cooling through boiling techniques on the performance of a PEMFC stack. The results showed that the coolant was able to absorb a maximum heat flux up to 3.2 W/cm^{-2}, which is much greater than that required by current PEM fuel cells. Cooling through

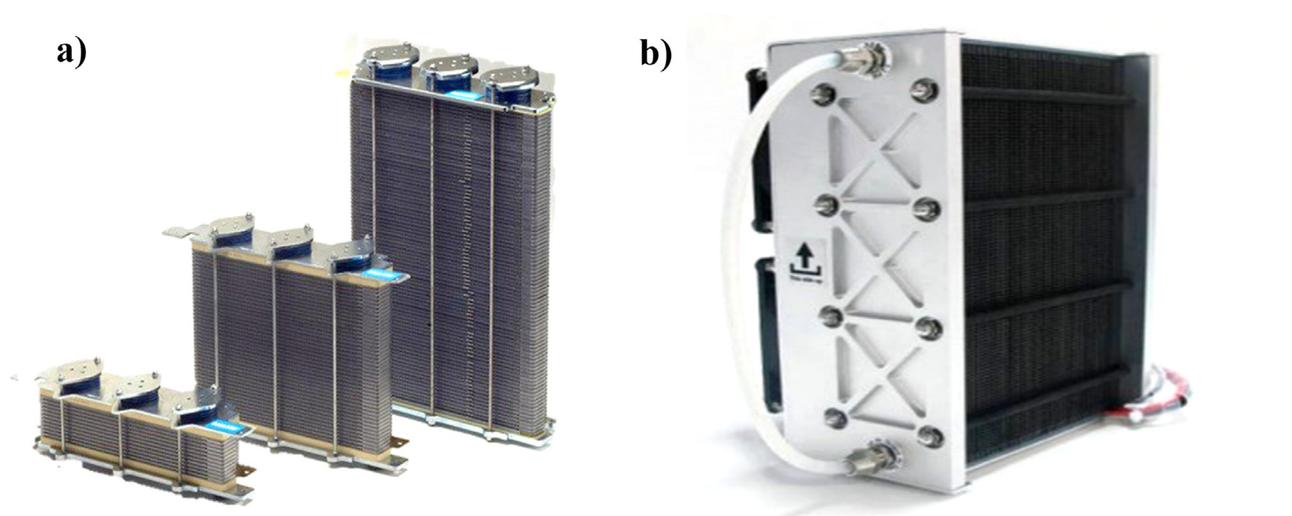

Fig. 4. a) 0.4–3.3 kW Ballard's FCgen®-1020ACS air-cooled fuel cell stacks [78]; b) 2 kW Horizon open-cathode H-Series PEM fuel cell stack [79].

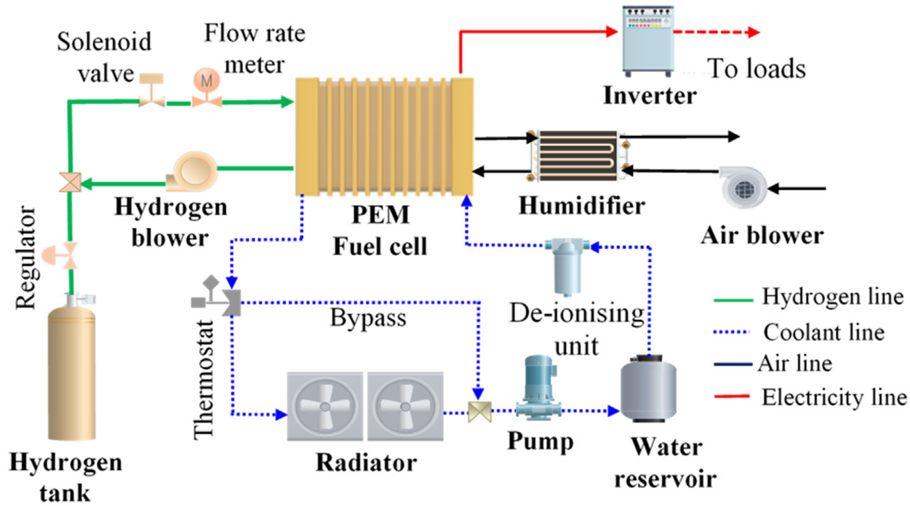

Fig. 5. Schematic demonstration of a typical liquid-cooled system used in PEMFCs.

water boiling can be applied for HT-PEMFC, which has operating temperature over 100 °C. Song et al. [104] developed a 1-kW PEMFC cooled by boiling water using buoyancy force to replace the coolant pump. It was shown that the stack temperature was not only kept stable but also distributed uniformly over the cells.

2.3. Opportunities for fuel cell heat recovery

The electrical energy efficiency of a PEMFC stack is in the range of ~30 to 55% depending mainly on its power output and operating conditions [33,105,106]. Most of inefficiencies of a fuel cell system appear in the form of heat to be normally rejected from the stack to maintain its temperature at a desirable level. Recovering this heat for onsite thermal applications helps improve the overall energy conversion efficiency of the system significantly. It is noteworthy that recovering this heat also offers an opportunity to reduce GHG emissions that would otherwise be released to the atmosphere if fossil fuels are used to meet such thermal demands [14].

In general, selecting the best technological options for waste heat recovery depends on operating temperature and the size of the system [107]. Heat recovery technologies for high-temperature (high quality) heat sources such as SOFCs, has been widely practiced for a range of applications as covered in comprehensive reviews published by Zhang et al., [108], Choudhury et al., [109], and Adam et al., [110]. On the other hand, heat recovery strategies for low-temperature heat sources (e.g. PEMFCs) is more challenging due to the low quality of heat generated, that is at approximately 60–80 °C for LT-PEMFC and ~120 to 180 °C for HT-PEMFC [15]. These low operating temperatures suggest several technical challenges and limitations in terms of the type of applications that can be considered for using the heat recovered from PEMFCs.

The coolant temperature can be significantly affected by the power generation and cooling condition. Although only low-quality heat can be recovered from low-temperature PEMFCs, the magnitude of heat

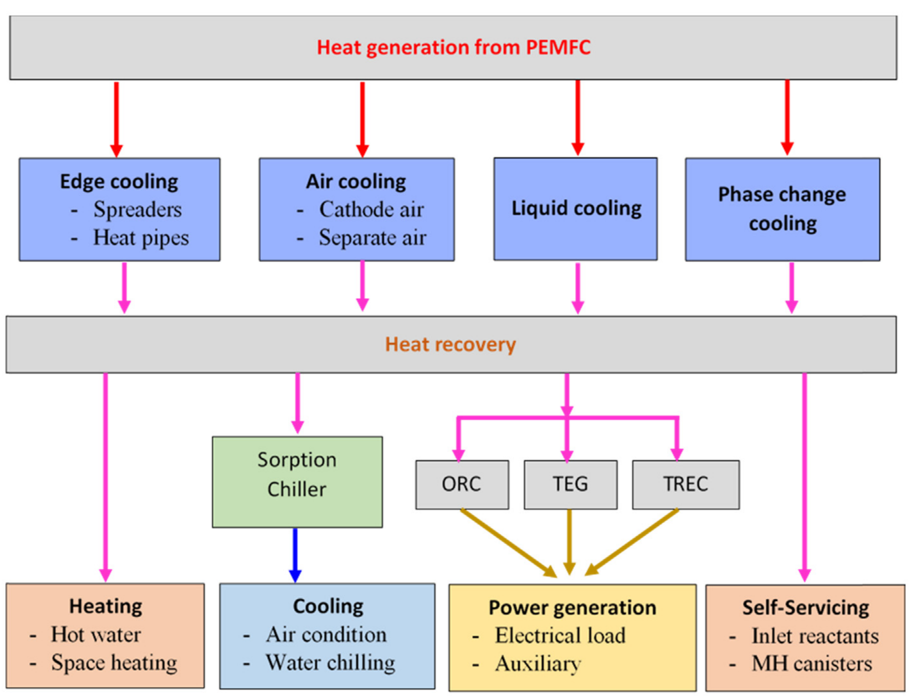

Fig. 6. Thermal management and heat recovery paths/options for PEMFC.

that can be captured from the coolant stream is usually significant that makes it worthwhile for recovery. At operating points close to the rated power of the PEMFC, this heat can be even equivalent to the electrical power output of stack. As briefly mentioned earlier the heat captured from the coolant stream of a PEMFC offers great opportunities to be used for small-scale low-temperature heating applications such as space heating and domestic hot water in CHP systems, preheating of inlet reactants, and thermal management of metal hydride hydrogen storage canisters [36]. Moreover, recent advances in heat recovery technologies allow for employing ORCs [47,111] and sorption refrigeration cycles [112,113] to be efficiently/effectively operated on the low-grade heat supplied by PEMFCs. Thermoelectric generators, which operate on the Seebeck effect, have been recently used for directly converting waste heat from PEMFCs to electricity, while the efficiency of this conversion is yet to increase significantly [114]. Fig. 6 presents different ways of capturing and utilising the low-grade heat available from PEMFCs. Each method will be discussed in detail in the following subsections.

3. Combined heat and power applications

Hydrogen can be supplied directly as pure hydrogen (e.g. onsite generation of hydrogen using renewables) or be extracted from hydrogen-rich fossil fuels such as natural gas through a reforming process as shown in Fig. 7. With the direct supply of hydrogen, the heat generated in the fuel cell itself is the only heat recovery opportunity offered by the system; however, in systems in which a hydrogen reformer is used the reformer also offers an additional opportunity for heat recovery. The present review, however, focuses only on heat recovery opportunities from PEMFC stacks.

3.1. *Isolated fuel cell systems*

Several studies have been conducted to date that investigated the feasibility of heat recovery from PEMFC stacks and its ability to improve the overall efficiency of the system in CHP cogeneration application. Briguglio et al. [31] experimentally investigated the possibility of heat recovery from a 5-kW PEMFC system to supply both electricity and heat (for hot water) in a typical Italian household. They found that the temperature of water can be increased to about 68 °C and the overall energy efficiency of the PEMFC-CHP system can reach up to 85% at maximum, when operating the fuel cell at its rated power. Similarly, by testing the potential for heat and power supply from a 500-W PEMFC stack, Shabani and Andrews [33,115] found that the overall energy conversion efficiency of the PEMFC can increase significantly from ~35 to 50% (in electricity generation mode alone) to up to 80% in combined heat and power mode of operation (i.e. for hot water supply). The experimental study on transient thermal and electrical energy efficiency of a PEMFC-CHP system, conducted by Hwang [116], also indicated an overall CHP efficiency of ~85%. In another experimental research by Hwang and Zhou [117], they found that by recovering heat from a 3-kW PEMFC it is possible to generate sufficient daily hot water demand for a typical family; and the rate of hot water supply increases linearly, from 40 l/min to 130 l/min, by increasing the power output of the stack from 0.5 kW to its rated power, 3 kW.

Operation conditions of a PEMFC can have significant impacts on its overall energy efficiency, when utilised in CHP mode. Hwang et al. [30,117,118] theoretically and experimentally studied the influences of operation parameters on the performance of a 5-kW commercial PEMFC used in CHP mode. They then reported that the electrical and CHP efficiency of the system increased by increasing the external load and pushing the fuel cell to its rated power (Fig. 8). A very similarity trend (i.e. the effect of power output on overall CHP energy efficiency) was reported by Shabani and Andrews [33]. In another study, Shabani [14] also reported that the stoichiometry of the input air and the fuel cell operating temperature are also two key factors affecting the overall efficiency of a PEMFC in heat and power generation. In another research by Saidi *et al.* [119], an exergy analysis was performed on a PEMFC-CHP system. They reported that by increasing the operating temperature of the fuel cell, the overall CHP efficiency of the system increases while increasing the air stoichiometry and fuel pressure can result in degrading its overall CHP efficiency.

3.2. *Renewable energy systems employing fuel cell heat recovery solutions*

Renewable energy systems (e.g. wind and solar) with hydrogen, generated onsite through renewables to store energy, have widely been considered and studied as promising solutions for uninterrupted power supply [6,120]. The key advantages of such systems compared to

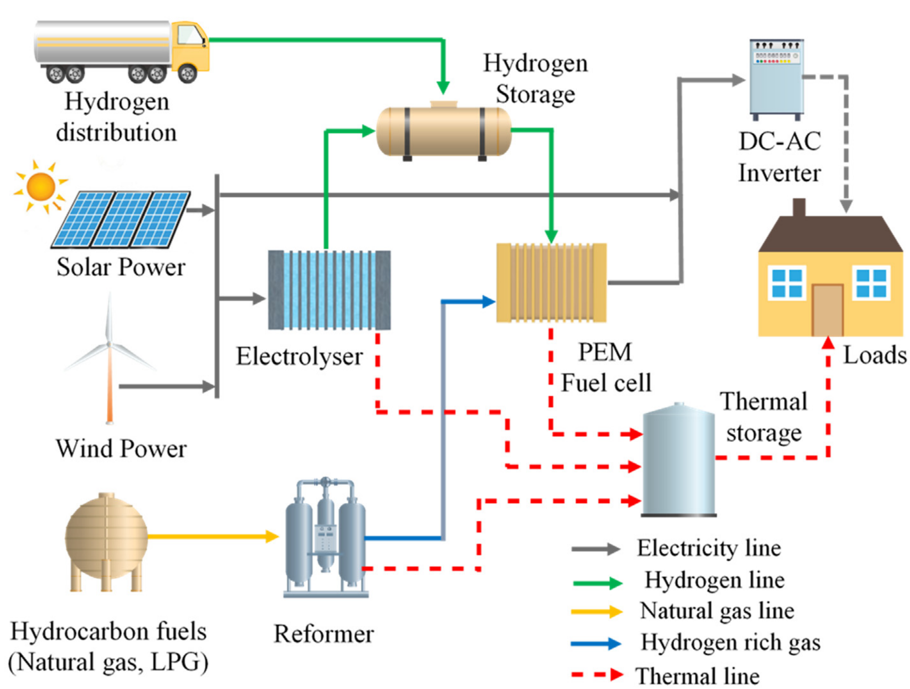

Fig. 7. Opportunities for heat recovery from a hydrogen reformer.

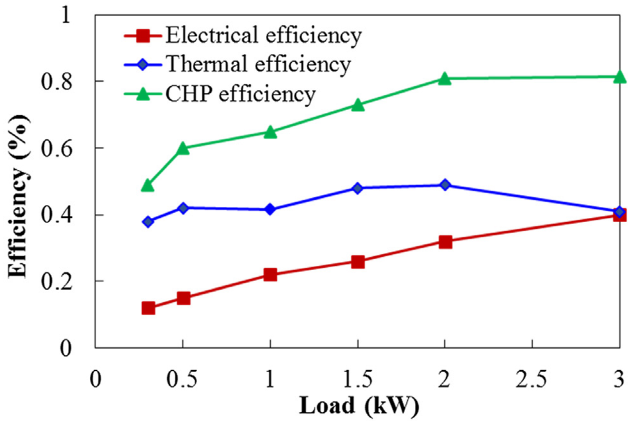

Fig. 8. The effect of external load on the efficiencies of the PEMFC-CHP system (reproduced from [117]).

conventional electrical power generation solutions, such as diesel generators, are their reliability, zero greenhouse gas emissions, complete standalone operation over extended periods of time, and low maintenance cost [115]. Furthermore, the overall round-trip energy efficiency of hydrogen-based solutions in applications with needs for long-term energy storage (i.e. season to season) is relatively better than batteries [121]. This is while batteries usually offer better round-trip energy efficiencies in short-term energy storage applications, particularly when they are not exposed to extreme hot/cold environments [122]. Hence, in long-term energy storage applications, using hydrogen for energy storage allows for installing smaller solar PV systems and eliminating backup diesel generators [33]. Many investigations have been reported on renewable energy solutions integrated with hydrogen systems for power generation, namely solar-hydrogen [33,123–129], wind-hydrogen [130–132], and wind/solar-hydrogen systems [133–135]. It is noteworthy that hydrogen systems are usually preferred solutions when it comes to large-scale energy storage applications [8].

A solar-hydrogen system, as schematically illustrated in Fig. 7, comprises a solar photovoltaic system, an electrolyser, a hydrogen storage solution, and a fuel cell system as its major components. The system should also have some balance of plants such as a control system, thermal management system, and electronics (DC/DC converter, load splitter, etc.). The PVs directly supply the load when possible and if there is any surplus, it is utilised by the electrolyser to generate hydrogen. This hydrogen is then stored in a tank and used by the fuel cell to generate electricity when the supply from the PVs is not enough to meet the demand [136]. Unlike when hydrogen-rich fossil fuels with fuel reforming technologies are used (i.e. to supply hydrogen to the fuel cell), hydrogen produced by the renewable-hydrogen systems has a high purity (up to 99.999%) [137], so issues related to CO poisoning are eliminated [138,139].

In practice, due to thermodynamic irreversibilities, water-splitting in the electrolyser is an exothermic process [140,141]. The heat generation from electrolyser (i.e. PEM electrolyser) accounts for around 30–40% of the power supplied as its efficiency is usually in the range of 55–70% based on LHV of hydrogen and depending on the pressure of hydrogen being supplied by the electrolyser [142]. However, about 30–40% of this heat is usually claimed by the electrolyser to preheat its feed-water and keep its operating temperature at about 70–90 °C. Then the remaining of this heat is rejected to the environment via the outer surface of the electrolyser and the gases produced [140]. This heat that is normally rejected from the electrolyser can be captured and used in on-site thermal applications. However, fuel cell in this system is the major producer of heat as discussed in detail before. Capturing this heat to meet part of the onsite thermal demands, is a key opportunity to enhance the overall round-trip energy efficiency of such renewable-hydrogen systems [5,33]

A PEMFC-CHP in a wind/solar-hydrogen system has been proposed by Lacko et al. [143]. In this study, the hot water demand for a typical household in Slovenia is served by utilising the heat recovered from the fuel cell, electrolyser, and excess electricity. The results showed that heat generation from electrolyser and fuel cell can annually supply over 51% of the total heat required, 18% of which accounted for the heat supplied by the electrolyser in the system and the remaining 33% supplied by the fuel cell. In another study, Pedrazzi et al.[144] developed a mathematical model of a wind-hydrogen CHP system in which metal hydride was used for storing hydrogen. In this model, the waste heat streams from the fuel cell stack, electrolyser, and MH canisters (i.e. during discharge) were captured and used for on-site thermal applications (i.e. hot water). By doing so, the overall energy efficiency of the system (in CHP mode) showed over 52% improvement compare to its efficiency in power only mode. It is noteworthy that recovering heat from the electrolyser was responsible for only a small portion of this improvement. Zafar and Dincer [145] conducted energy and exergy analysis on a hybrid photovoltaic/thermal (PV/T)-fuel cell model for electricity, space heating, and water production. They concluded that when heat generated by fuel cell stack is utilised, the overall energy conversion efficiency, which is defined as the ratio of energy outputs (i.e. heat and power consumptions) and the input energy supplied by renewable energy (i.e. solar power), could increase from 2.4% to 5.65%, and the overall exergy efficiency raised from 2.8% to 19.8%.

The overall energy conversion efficiency (i.e. solar radiation to electricity) of a renewable energy-hydrogen employing PEMFC-CHP system is very low (i.e. under 6% for solar-hydrogen [145] and 12.5% for wind-hydrogen [144]). This is mainly due to the low energy efficiency of the power generation unit (e.g. the PV system and wind turbine), as described in the Eqs. (5) and (6) , respectively:

$$\eta_{PV-CHP} = \frac{Q_{PV-load} + Q_{FC} + Q_{Re,FC} + Q_{Re,EL}}{Q_{SPV}} \tag{5}$$

$$\eta_{wind-CHP} = \frac{Q_{wind-load} + Q_{FC} + Q_{Re,FC} + Q_{Re,EL}}{Q_{WT}} \tag{6}$$

where Q_{SPV} is the total solar energy on titled solar panels over a period time (i.e. daily or yearly), (kJ); Q_{WT} is total wind energy on wind turbines, (kJ); $Q_{PV-load}$, $Q_{wind-load}$ and Q_{FC} are the electrical energy delivery to load (not including electrolyser) by PV, wind turbine and fuel cell over a period time respectively, (kJ); $Q_{Re,FC}$ and $Q_{Re,EL}$ are thermal energy recovered from fuel cell and electrolyser respectively, (kJ).

Focussing on the energy storage part of the system, the roundtrip energy efficiency of the storage system is defined by excluding the performance of PVs and/or wind turbines. Eq. (7) describes the round-trip energy efficiency of a hydrogen-based energy storage system when fuel cell and electrolyser heat recovery is taken into consideration. Without considering the heat recovered from the fuel cell and electrolyser, the equation should be modified as in Eq. (8).

$$\eta_{RT-CHP} = \frac{Q_{FC-load} + Q_{Re,FC} + Q_{Re,EL}}{Q_{EL}} \tag{7}$$

$$\eta_{RT} = \frac{Q_{FC-load}}{Q_{EL}} \tag{8}$$

In these equations η_{RT} and η_{RT-CHP} are the round-trip energy efficieny of hydrogen based energy storage system without and with heat recovery applications respectively; $Q_{FC-load}$ is the electrical energy distributed to load by fuel cell, (kJ); and Q_{EL} is electrical energy received by electrolyser, (kJ).

One of the hurdles facing hydrogen-based energy storage systems is its low round-trip energy efficiency (around 20–40%) [137,146], that limits their applicability to long-term energy storage applications. However, by recovering heat from the fuel cell stack for CHP applications (i.e. domestic hot water), the overall round-trip energy efficiency of the hydrogen storage system can be improved significantly, up to about 50% [33,147].

Another drawback of such hydrogen-based energy storage solutions is their relatively high capital cost. Hence, optimal sizing of the system would play a critical role in reducing the overall cost of the system [115,148]. Furthermore, because of the intermittency and variation of the input energy (i.e. solar radiation or wind speed variations), the matching of system's power outputs and the load demands during the operation should be considered when designing and optimising such systems [149]. The economics of the system [115,148,150] and its energy efficiency (i.e. electrical and thermal efficiency) [115,151,152] are the key objective functions usually used to optimise renewable hydrogen systems employing PEMFC-CHP arrangements.

PEMFC-CHP systems have been proven to be a technically feasible solution to supply heat and power in residential applications [33,153]. However, the heat extracted from the fuel cell (i.e. normally sized to fully meet the electrical demand), can partially meet the thermal demand of the application [14]. For example, in a solar-hydrogen CHP system, the heat extracted from the fuel cell is sufficient to meet about 40–50% of total thermal energy required for hot water supply in a domestic remote application. [33,154]. Hence, a gas or electric booster is required to fill in the gap to fully meet the thermal demand of the building [110,155–157]. However, the use of such boosters would then contribute to the emission of greenhouse and other harmful gases.

Other renewable energy inputs can though be considered to cover the supply gap and fully meet the heat demand (i.e. without using fossil fuels). In line with this idea, a novel idea for integration of a solar-hydrogen CHP system with solar-thermal collectors to supply both electricity and hot water for a standalone application was proposed and investigated by Assaf and Shabani [151,152,158,159]. The schematic of this integrated hybrid renewable energy CHP system is shown in Fig. 9. In this configuration, the solar-thermal collectors operate in a complimentary way with the heat recovery unit of the PEMFC. The key advantage of this arrangement is that, the period when the output from the solar-thermal collectors is not enough to meet the thermal demand of the building (e.g. for hot water) usually coincides with the time that the fuel cell (in the solar-hydrogen CHP system) starts operating, generating heat and power. This is usually the period that the output of the PVs is not also enough to meet the electrical demand of the building, that is why the fuel cell must kick in to fill in the gap of supply (i.e. from the PVs). This novel idea was initially explored using the same case studied earlier by Shabani [14] for investigating the feasibility of the idea of solar-hydrogen CHP system for standalone applications. A mathematical model was developed in TRNSYS and applied on this case that was assumed for a conservative passive off-grid household in southeast Australia with 5 kWh/day electrical demand peaked at 0.3 kW [152]. It was found then for an optimally-sized configuration, this integrated system could meet ~95% of the annual hot water demand (i.e. with still 5% unreliability for heat supply).

Later on, Assaf and Shabani [49] proposed a modified version of their idea to cover this 5% of gap and achieve 100% reliability to supply heat for hot water throughout the year. Their simple solution included the addition of a little inline electric heater running on the PVs or fuel cell. Interestingly, their modified integrated solution did suggest a very insignificant increase in the size of the PV system and the levelised cost of energy supplied (i.e. per kWh). In terms of economic performance of system, their study [158] indicated 0.4 US$/kWh for the cost of energy (i.e. for their solar-hydrogen CHP integrated with solar thermal collector), which was competitive with traditional power and heat solutions employing gasoline generator for power and natural gas hot water supply.

4. Combined cooling, heating, and power applications

Sorption cooling cycles utilise heat sources (e.g. solar thermal, flue gas and waste heat from fuel cells) to provide the required energy for increasing the pressure of refrigerant in a cooling process [160,161]. Recent advances in absorption (liquid-vapour pairs) and adsorption (solid-vapour pairs) technologies allow such systems to exploit the required heat from low-temperature heat sources in the range between 50 °C and 100 °C [162,163]. Considering the operating temperature of PEMFCs (e.g. 60–80 °C for LT-PEMFCs) the heat recovered from a PEMFC is a promising input for CCP or CCHP applications.

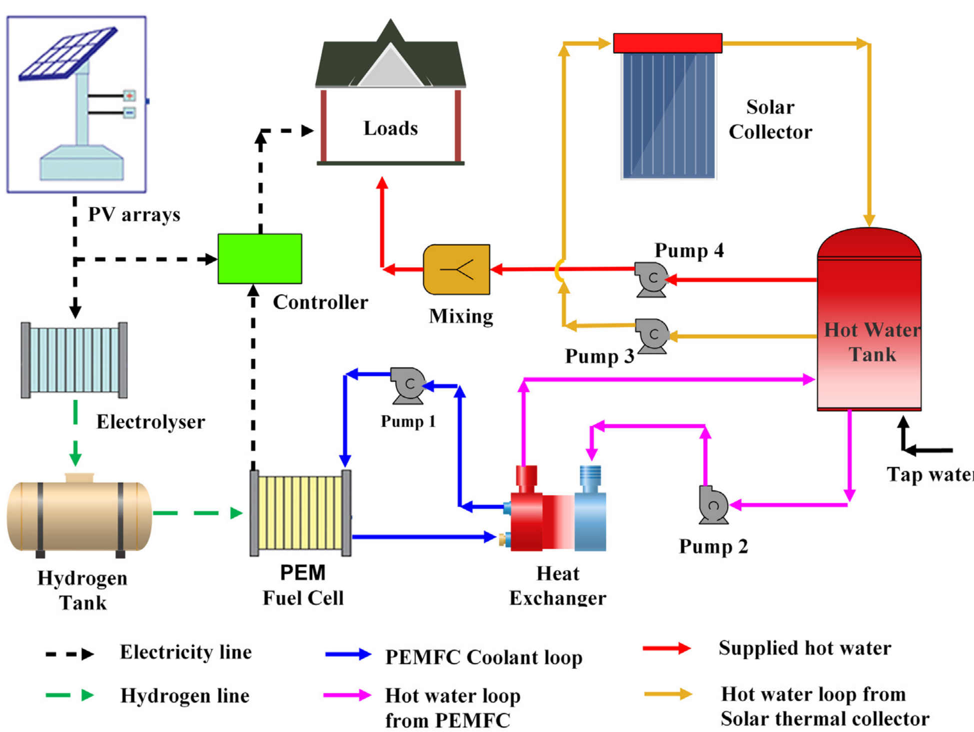

Fig. 9. Schematic diagram of standalone solar hydrogen CHP system integrated with solar thermal collectors (reproduced from [158]).

4.1. Sorption refrigeration technologies integrated with fuel cell systems

Table 2 indicates the refrigerant pairs and its typical characteristics used in the sorption refrigeration technologies, which can be integrated with PEMFCs for CCP/CCHP applications. Common conventional absorption chiller systems using lithium bromide-water (LiBr-water) as absorbent-refrigerant pairs (LiBr as absorbent and water as refrigerant) and water-ammonia (water-NH_3) can be powered by heat sources at 120–170 °C to yield COPs of about 0.5–0.7. The double-effect chillers based on such pars can improve the coefficient of performance (COP) (i.e. up to 1.2), but it requires the heat sources temperature to be at 120–170 °C [164,165], which is matching the operating temperature range of HT-PEMFCs. The absorption refrigeration using water-NH_3 could be powered by the heat sources from 80 to 200 °C to provide a cooling effect (i.e. glycol water) down to sub-zero temperature with the COP of 0.2–0.6. The adsorption chiller systems based on solids-vapour pairs such as silica gel-water, zeolite-water and activated carbon-methanol is most suitable for LT-PEMFC heat recovery because they require the source of heat input to be at a temperature in the range of 60–120 °C to operate [166–168].

4.2. Absorption refrigeration

Depending on the absorbent-refrigerant solution pairs used, the waste heat from PEMFCs can be utilised to drive the absorption chiller systems for different cooling purposes.

The typical configuration of an absorption chiller system running on fuel cell heat is shown in Fig. 10. The hot liquid coolant exiting the PEMFC subsystem enters directly into the generator of the absorption cooling system, where the heat is captured and used to desorb the refrigerant out of absorbent. The refrigerant exiting the generator under vapour form then flows through the rest of the refrigeration cycle including condenser, expansion valve and evaporator.

Recently, several studies on recovering this low-grade heat to drive the generator of absorption refrigeration systems for CCP or CCHP applications, have been reported as summarised in Table 3.

The cooling capacity generated by absorption chillers based PEMFC systems can account for from around 50% to 95% the power generation of fuel cell stacks. For example, Pilatowsky et al. [169] developed a mathematical model based on a 1-kW PEMFC integrated with monomethylamine-water (MMA-water) absorption air conditioning. By recovering heat from the fuel cell stack at its rated power, the chiller could generate 0.44–0.57 kW of cooling capacity. In another study, Yang and Zhang [173] numerically investigated the performance of a hybrid system by integrating a PEMFC with an absorption refrigerator to simultaneously produce electricity and cooling. They could then show that it is feasible to capture waste heat from a PEMFC to drive absorption air condition systems for combined air cooling and power applications.

The overall the efficiency of the fuel cell can though be enhanced significantly when the heat generated by the fuel cell is captured and used for cooling purposes. To quantify this performance enhancement, Chen et al. [89] conducted parametric studies on a cogeneration cooling heating and power system incorporating LT-PEMFC stack with a single-effect Lithium Bromide-water (LiBr-water) absorption chiller. They found that the maximum energy efficiency of their system could reach around 70% and 82% in summer and winter respectively. Chahartaghi & Kharkeshi [171] also investigated the performance of a CCHP system based on single-effect water/LiBr absorption chiller and PEMFC as a prime mover. They found that the COP of the chiller and overall energy efficiency of the CCHP system increased by increasing the power output of fuel cell stack, as illustrated in Fig. 11. The results also indicated that an energy efficiency of maximum 84.5% could be achieved for this CCHP system.

The quality of the heat (i.e. determined by its temperature) supplied to generator is an important consideration for selecting the absorbent-refrigerant solution pairs. In fact, it can also significantly affect the cooling capacity and COP of the absorption chiller systems such that by increasing the temperature of the heat source, higher COPs can be achieved. By taking this effect into account, Chen et al. [172] proposed a novel system in which a parabolic trough solar collector (PTSC) into cooling loop was added to the system to boost up the heat recovered from a LT-PEMFC and achieve 165 °C of temperature for driving a double-effect absorption chiller. The fuel cell employed in this system could deliver energy (i.e. heat and power) at an overall energy conversion efficiency of 80.5%. Arsalis [164] proposed a theoretical model to simulate a 100-kW_e hybrid HT-PEMFC (operating in the range of 140–160 °C) with two different absorption chiller system configurations: (i) a double-effect water-LiBr subsystem for cooling water at 5–10 °C; and (ii) a single-effect NH_3-water for cooling brine or glycol water at −60 to 0 °C. At maximum power output of the PEMFC (i.e. 100 kW), the heat recovered from the stack could satisfy the cooling capacities of up to 128 kW and 64.5 kW for double-effect water-LiBr and single-effect NH_3-water refrigeration subsystems, respectively.

In terms of economic benefits of such systems, Arsalis [164] illustrated that despite the relatively-high capital cost of such combined cooling-power PEMFC solutions, such integrated systems can still show economic attractions due to their low running costs and the saving introduced by the heat recovered from the fuel cells. They also indicated that the capital cost of such systems has experienced a significant drop in recent years, a trend that is continuing.

Overall, it can be seen that a high-temperature heat source such as that from HT-PEMFC stacks is very promising for driving absorption chiller systems. Hence, the heat recovery opportunities from these stacks should be further researched and developed for cooling applications.

Table 2
Characteristics of sorption refrigeration technologies using PEMFC heat [165].

Refrigerant pairs (absorbent-refrigerant)	Heat source temperature (°C)	Cooling Capacity (kW)	Refrigeration output	COP	Heat sources from FC
LiBr-water absorption					
Single-effect	70–90	5–7000	5–10 °C chilled water	0.5–0.7	LT-PEMFC liquid cooling
Double-effect	120–170	20–11,000	5–10 °C chilled water	1.0–1.2	HT-PEMFC liquid cooling
Water-NH3 absorption					
Single-effect	80–200	10–90	5–10 °C chilled water	0.5–0.6	LT and HT-PEMFC liquid cooling
Single-effect	100–200	10–6500	−60 to 0 glycol water	0.2–0.6	HT-PEMFC liquid cooling
Silica gel-water adsorption	60–85	5–1000	7–15 °C chilled water	0.3–0.7	LT-PEMFC liquid cooling
Activated Carbon-methanol or CaCl2-NH3 adsorption	80–120	1–12	Ice making or −10 glycol water	0.1–0.4	LT-PEMFC and HT-PEMFC liquid cooling
Solid desiccant cooling	60–150	1–5	18–26 °C air cooling	0.3–1	LT-PEMFC and HT-PEMFC liquid cooling
Liquid desiccant cooling	61–110	50–500	18–26 °C air cooling	0.5–1.2	LT-PEMFC and HT-PEMFC liquid and air cooling

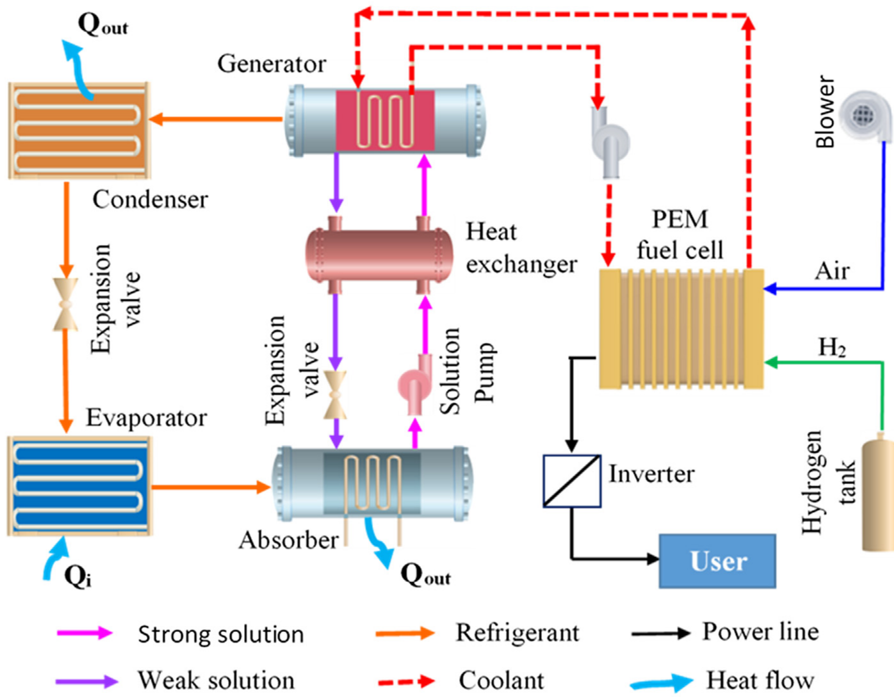

Fig. 10. Schematic illustration of PEMFC heat recovery arrangement for an absorption chiller system.

4.3. Adsorption refrigeration

As discussed earlier in Section 4.1, most of adsorption chillers, which employ solid-vapour pairs, can work by heat sources below 80 °C; thus, they are most suitable for integration with LT-PEMFC systems. Table 4 summaries the recent studies on LT-PEMFC integrated with adsorption cooling cycles for CCP applications. The COP of PEMFC-based adsorption cooling systems and overall energy efficiency of the PEMFC used in such cycles are around 0.2–0.45 and 60%-65% respectively, which are lower than when the fuel cells are integrated with absorption cooling cycles.

Oh et al. [38] analysed the effects of desorption temperature on the performance of silica gel-water and activated carbon fibre (ACF)-ethanol adsorption cooling system driven by waste heat from a LT-PEMFC and a SOFC. Their results showed that cooling capacities and COP values of both such adsorption cycles utilising waste heat from SOFC are 2.2 and 1.2 times respectively higher than when waste heat from the LT-PEMFC is utilised.

Recently, Oro et al. (2018) [88] experimentally investigated the of heat recovery from a 1400-W of PEMFC stack to drive a chemisorption chiller system in which newly-developed adsorption pairs of NaBr impregnated in expanded graphite as adsorbent and NH_3 as refrigerant are employed. The system was used for both electricity and cooling effect supply. The results showed that with the stack power output in the range of 600–1400 W, the cooling capacity of the chiller subsystem could reach up to 400 W that led to increasing the overall energy conversion efficiency of the system to 63%.

5. Integration with other power generation systems

The PEMFC heat recovery can be applied for power generation by integration with systems organic Rankine cycles, thermoelectricity generators, and thermally regenerative electrochemical cycles.

5.1. Organic rankine cycles

Organic Rankine cycles (ORCs) work on the same principle of steam Rankine cycles to generate electricity from thermal energy, but it utilises low boiling point organic working fluids to recover waste heat from low-grade (i.e. low temperature) heat sources [174]. Working fluids deployed in ORC arrangements allow them to operate at temperatures ranging from 65 °C to 200 °C [111,174,175]. ORCs have been widely employed for low-temperature heat into electricity for different applications. This includes using waste heat (e.g. from a fuel cell) or heat supplied by solar thermal and geothermal systems or surface seawater [176]. Schematic of such hybrid power systems with an ORC used to recover heat from a PEMFC is shown in Fig. 12.

The thermodynamic properties of the working fluid used in the ORC system have significant impacts on the system efficiency, operating conditions, environmental impact, and economic viability of such arrangements [111,174]. A suitable working fluid must meet both required thermophysical properties for applications and adequate chemical stability within the desired range for the operating temperature. Possible working fluids that can be employed in ORC to exploit the low to medium grade heat recovered from LT and HT PEMFCs can be found in the literature [111,177]; however, Butane, Propane, R123, R245fa and R134a are among the most common working fluids used for this purpose. They can be used for evaporator operating temperatures in the range of 65–250 °C to achieve thermal energy efficiencies in the range of [111,178]. Table 5 summaries the popular working fluids used in ORC based PEMFC heat recovery systems.

Explaining the performance indicators used in Table 5, the performance of the PEMFC integration with ORC system is usually evaluated by the thermal efficiency of ORC system (η_{ORC-th}) and overall electrical energy efficiency ($\eta_{ORC-elec}$) of the combined fuel cell systems and ORC. These are though calculated using Eqs. (9) and (10) [19].

$$\eta_{ORC-th} = \frac{P_{turb} - P_{pump}}{\dot{Q}_{FC-cooling}} \tag{9}$$

$$\eta_{ORC-elec} = \frac{P_{FC} + P_{turb} - P_{pump}}{\dot{m}_{H2}.\ HHV_{H2}} \tag{10}$$

In these equations, P_{turb} are power generated by turbine in the ORC system (W); $P_{pump}$is power consumption by pump (W); P_{FC} is the power output of the fuel cell; and $\dot{Q}_{FC-cooling}$ is the cooling load of the fuel cell supplied to the ORC.

Table 3
Recent researches on the integration of PEMFC with absorption chillers.

Fuel Cell	Fuel cell operating temperature	Refrigerant pairs	COP	Overall Efficiency	Cooling energy generation (kW)	Purposes	Ref
1 kW LT-PEMFC	60–80 °C	monomethylamine/water (MMA/water)	0.4–0.7	NA	0.44–0.57	CCHP	[169]
5 kW LT-PEMFC	75–85 °C	water/Lithium Bromide (LiBr) single-effect	0.7	68.1%	4.8	CCHP	[89]
6 kW LT-PEMFC	67 °C	water/LiBr Half effect	0.425	61%	0.4–2.8 for CCP, 0.33–1.97 for CCHP	CCP and CCHP	[170]
40 kW LT-PEMFC	80 °C	water/LiBr single-effect	0.4–0.8	84.55%	NA	CCP	[171]
100 kW HT-PEMFC, oil cooling	140–160 °C	water/LiBr double-effect	1.2	NA	128	5–10 cooling water	[164]
100 kW HT-PEMFC, oil cooling	140–160 °C	NH3/water single-effect	0.6	NA	64	−60 to 0 cooling brine or glycol	[164]
5 kW LT-PEMFC	85 °C	water/LiBr double-effect	NA	80.50%	60 (assisted by 42 kW PTSC)	CCHP	[172]

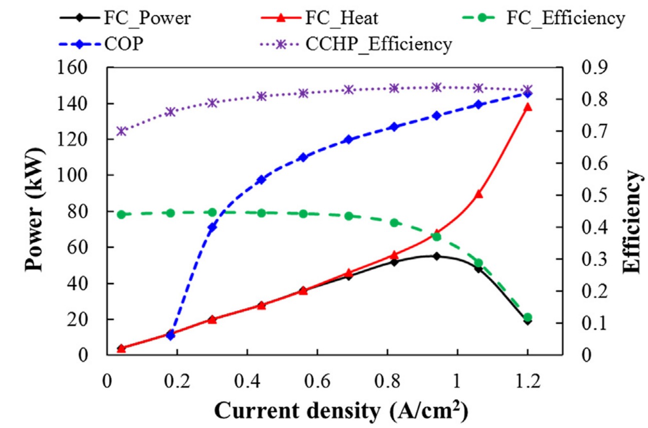

Fig. 11. The performance of a PEMFC-based CCHP systems (reproduced from [171]).

He et al. [39] theoretically investigated thermodynamic feasibility of PEMFC (operating at 60 °C) heat recovery to run an ORC and a heat pump combined ORC (HPORC). By considering several potential working fluids (i.e. R123, R245fa, R134a, water and ethanol), they found that the best thermal energy efficiency (i.e. for the cycle) was only 4.03% obtained for an ORC in which R245fa was used as the working fluid. Meanwhile, the best performance of 4.73% for the HPORC was achieved by utilising R123. They also concluded that the presence of heat pump improved the ability of the system for recovering the PEMFC heat.

In another study, a mathematical model of a hybrid PEMFC and ORC system for power cogeneration was developed by Zhao et al. [19]. The model was used for investigating the impacts of key operating parameters such as fuel flow rate, fuel cell operating pressure, turbine inlet pressure, and turbine backpressure, on thermal energy efficiency of the ORCs for converting heat recovered from the PEMFC into electricity. A 1200 kW PEMFC stack and 140 kW ORC system were then simulated by the model with five different working fluids (i.e. R245fa, R245ca, R236fa, R123, Isobutane). The impacts of hydrogen flow rate and fuel cell operating pressure on the performance of PEMFC based ORC system are shown in Fig. 13. The results from this study also indicated that by recovering heat from the PEMFC at different operating points (i.e. 1000 kW and 1200 kW), the efficiency of the hybrid integrated PEMFC/ORC system could be improved by over 13% compared to that provided by only the PEMFC stack.

From thermodynamic viewpoint, the efficiency of a Rankine cycle is higher when the temperature difference between the hot reservoir and cold environment is larger. Because most ORC systems are operated in atmospheric environment (i.e. rejecting heat through their condenser), the larger different temperature is usually obtained by increasing the temperature of the heat flow supplied to the evaporator. Hence, HT-PEMFCs operating at 120–200 °C, can even be more suitable candidates for running ORCs. Lee et al. [40] developed an analytical model to optimise the overall power generation and efficiency of a hybrid HT-PEMFC/ORC system. The results indicated that the electricity efficiency of the hybrid system when the fuel cell stack operates at 20% of its capacity and 160 °C is 6% larger than that can be provided by the PEMFC only. This value increased to 7% when the power output of the stack increased to 40%. Furthermore, they pointed out that by increasing the operating temperature of the PEMFC stack from 160 °C to 180 °C, at 20% of stack capacity, the energy efficiency of the whole system increased by further 2%. Similarly, by considering thermodynamic and economic optimisation criteria, Perna et al. [87] developed a numerical model, which was able to use the heat from a HT-PEMFC for CHP applications (i.e. electric and hot water) or in an ORC for power generation (i.e. in parallel with the PEMFC). The impacts of different operating conditions of ORC subsystem such as evaporation

Table 4
Recent researches on the integration of PEMFC with adsorption chillers.

Fuel Cell	Fuel cell operating temperature (°C)	Refrigerant pairs	COP	Overall Efficiency %	Cooling capacity (kW)	Purposes	Ref
1 kW LT-PEMFC	65	activated carbon fibre (ACF)/ethanol	0.2–0.45	60	0.1	CCP	[38]
1 kW LT-PEMFC	65	Silica gel/water	0.25–0.55	64	0.18	CCP	[38]
1.4 kW LT-PEMFC	65–75	NaBr impregnated in expanded graphite/NH3	0.2–0.3	63	0.4	CCP	[88]

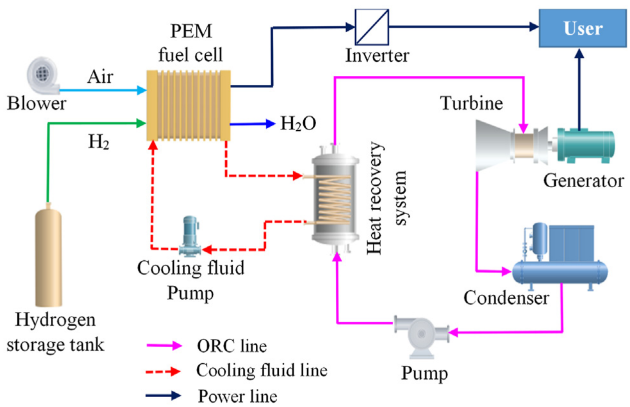

Fig. 12. Schematic diagram of hybrid PEMFC heat recovery driving ORC.

pressure, condensation temperature, heat transfer efficiency and turbine efficiency on the performance of the hybrid system were investigated. The results showed that the net efficiencies of the ORC running on the fuel cell waste heat were 8.1% and 8.6% for R142 and R245FA working fluids, respectively. The overall energy efficiency in CHP mode and power generation mode (i.e. by the PEMFC and the ORC) were found to be 79% and 43% respectively.

5.2. Thermoelectricity generators

Recent major advancements in semi-conductive materials have resulted in extensive application of thermoelectric generators (TEGs) in waste heat recovery applications. TEG is a device that directly converts heat into electricity through the Seebeck effect. The use of TEGs in waste heat recovery systems has several advantages such as silence operation, being of small size with no moving parts, offering high durability, environmental friendliness, and ability to convert low quality thermal energy into electricity [182]. Therefore, TEGs have been considered as an attractive option to improve the overall energy conversion efficiency of systems with available low-grade heat sources while offering reliability and design flexibility: e.g. geothermal heat and solar-thermal systems, exhaust gas from automotive, industrial waste heat processes [183,184].

A standard single-stage thermodynamic module is able to work with temperature difference up to 80 °C with hot plate temperature of 60–180 °C [185]. Hence, by considering the same operating temperature range of PEMFC stacks, the integration of TEGs into PEMFC system (i.e. to exploit the generated heat for further electricity generation) is seen as an option for improving the overall energy efficiency of the fuel cell system [18,186–190]. Fig. 14 shows the schematic diagram of a typical PEMFC and TEG hybrid system for power cogeneration. The hot side of the TEG receives the heat from the coolant leaving the stack (i.e. via an external heat exchanger), while the cold side is cooled down by being exposed to the ambient. The TEG converts the waste heat received from the coolant into electricity due to the temperature difference between its hot and cold side. The coolant is though cooled down before returning to the PEMFC stack.

The magnitudes of thermoelectric voltage and power output depend on the temperature difference between hot and cold plates, external load resistance, and assembled semi-conduction materials [192]. The performance of a TEG is also affected by thermocouple material properties, which is known as thermoelectric figure of merit (ZT), including the Seebeck coefficient, absolute temperature, electrical and thermal conductivity. The expression for dimensionless ZT is given by the following equation:

$$ZT = \frac{S^2\sigma T}{k} \tag{11}$$

where S is the Seebeck coefficient, (V/K); σ is the electrical conductivity of thermocouple material, (S/m); k is the thermal conductivity of thermocouple material, (W/mK); and T is the absolute temperature, (K).

The power generation by a TEG (P_{TEG}) can be calculated by applying

Table 5
Studies on PEMFC heat recovery for running ORCs.

Fuel Cell	Fuel cell operating temperature	Fuel cell power generation	Fuel cell Efficiency	Organic working fluids	ORC efficiency	Overall system efficiency	Improvement percentage	Ref
2.5 kW HT-PEMFC	160 °C	2.5 kW	40%	R142b	10.1%	43.1%	7.8%	[87]
				R245fa	10.7%	43.3%	8.3%	
1.2 kW LT-PEMFC	85 °C	1 kW	37.59%	R245fa	10.6%	42.7%	13.5%	[19]
				R245ca	10.7%	42.7%	13.7%	
				R236fa	10.0%	42.4%	12.7%	
				R123	10.9%	42.8%	14.0%	
5 kW LT-PEMFC	60 °C	5 kW	NA	R134a	4.6%	NA	–	[39]
				R123	5.6%	NA	–	
				R245fa	5.8%	NA	–	
1180 kW LT-PEMFC	85 °C	1180 kW	NA	R245fa	6.5%	44.0%	–	[179,180]
1100 kW LT-PEMFC	80 °C	752 kW	30.60%	R245fa	NA	34.8%	13.6%	[181]
				R123	NA	34.9%	14.0%	
				i-Butane	NA	34.6%	13.0%	
				n-Pentane	NA	34.8%	13.8%	

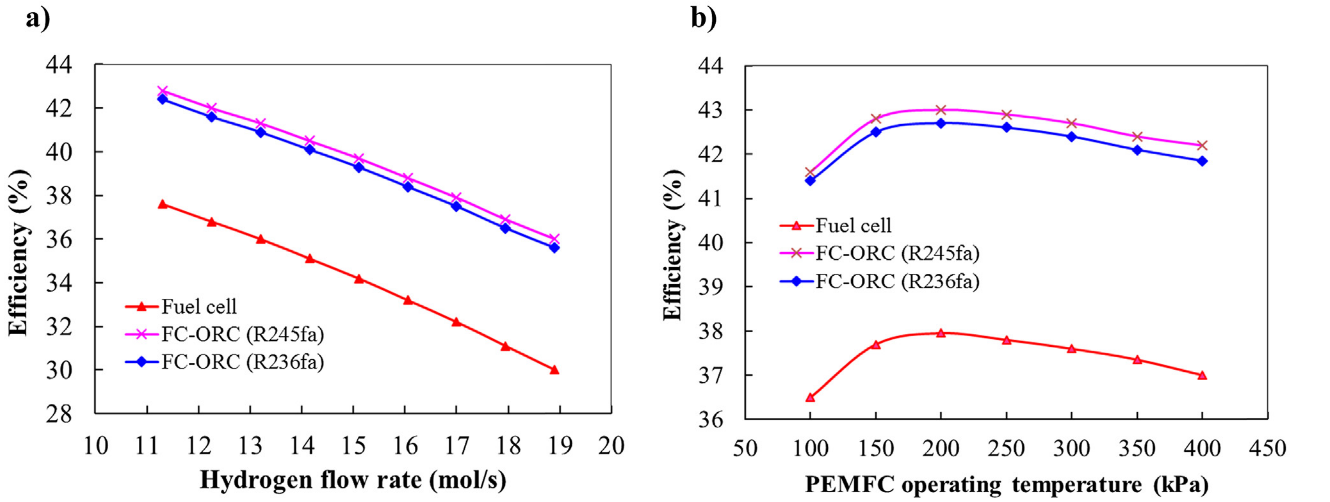

Fig. 13. The effects of operating parameters on the performance of PEMFC based ORC system; a) effect of hydrogen flow rate; b) effect of fuel cell operating pressure (reproduced from [19]).

the energy balance on the TEG module as follows [41]:

$$P_{TEG} = Q_H - Q_C = S(T_H - T_C)I - R_{TEG}I^2 \tag{12}$$

where Q_H and Q_C are the heat transfer rate in the hot and cold side of TEG module, (W); T_H and T_C are the temperature of the hot and cold sides, (°C); I is the output current generated by TEG, (A); and R_{TEG} is the electrical resistivity of the TEG module, (Ω).

As given by Eq. (13), the maximum energy efficiency (η_{TEG}) of a TEG module is a function of the dimensionless ZT, the temperatures of hot side (T_H) and cold side (T_C) [41,193]. Eq. (14) also provides the overall energy efficiency (η_{FC-TEG}) of the PEMFC integrated with the TEG system:

$$\eta_{TEG} = \frac{T_H - T_C}{T_H}\cdot\frac{\sqrt{1+ZT}-1}{\sqrt{1+ZT}+\frac{T_H}{T_C}} \tag{13}$$

$$\eta_{FC-TEG} = \frac{P_{FC} + P_{TEG}}{\dot{m}_{H_2}.\ HHV_{H2}} \tag{14}$$

The term $\frac{T_H - T_C}{T_H}$ in the Eq. (13) is representing the Carnot efficiency of a thermodynamic system operating between T_H and T_C. Similar to other power generation thermodynamic cycles, the efficiency of TEGs is limited by Carnot efficiency and a typical TEG works at about 20% of the Carnot efficiency over a wide temperature range [182]. At the same temperature difference, by increasing the ZT value of the TEG its energy efficiency improves. In the operating temperature range of PEMFCs (i.e. 60–200 °C), most currently commercial thermoelectric modules have ZT values less than 1 with some of them being up to around 1.5 [185]. Any TEG module with ZT value above 1 is considered to be good; however, the ZT value should be above 3 to make this heat recovery technique techno-economically viable [185].

Sulaiman et al. [194,195] experimentally and theoretically studied heat recovery model of a 2-kW an open-cathode PEMFC in which the fuel cell heat was used by a heat pipe assisted a TEG module for co-electricity generation. The performance of TEG module in the system was investigated at different loads of the fuel cell stack, TEG orientations and convection mode configurations. The results showed that a single TEG unit can generate approximately 218 mW of maximum electrical power at 1 kW of PEMFC power. Chen et al. [18] also developed a new model of a hybrid PEMFC, TEG system for power

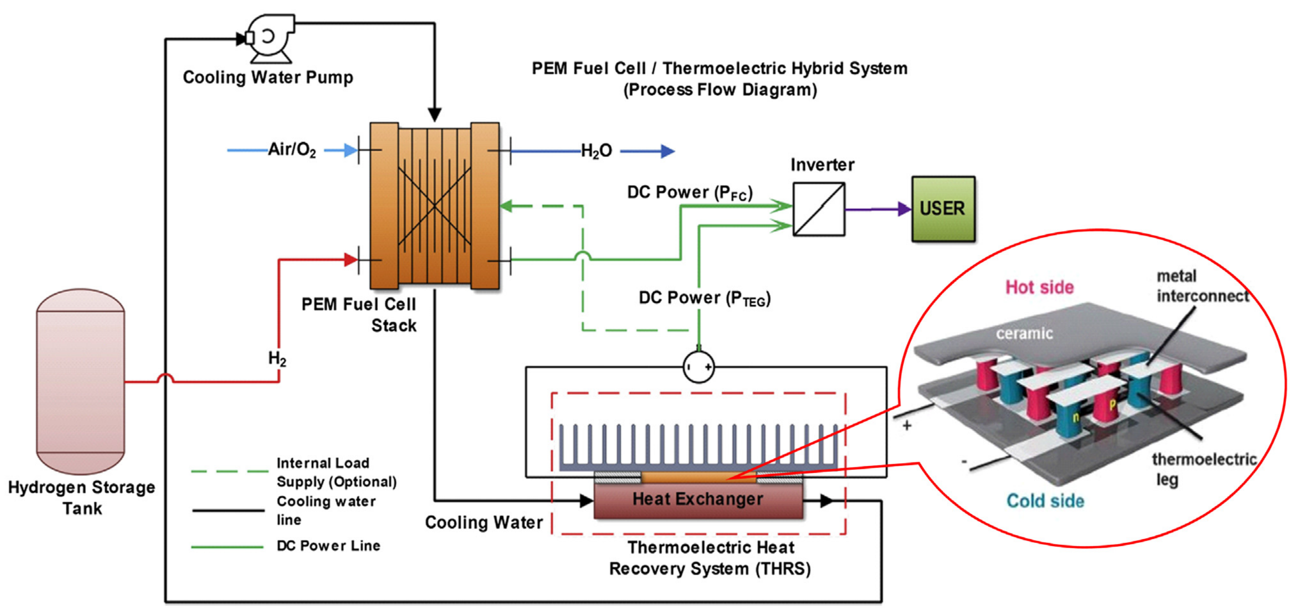

Fig. 14. Schematic diagram of a hybrid PEMFC and TEG (reproduced from [41;191]).

cogeneration. The results indicated that the maximum power output density of the system increased from 0.32 W/cm^2 for PEMFC stack only to 0.36 W/cm^2 for cogeneration with TEGs, resulting in over 12% improvement in the system's electrical energy efficiency (Fig. 15). They also reported that the operating conditions of the PEMFC used in their model (i.e. operating temperature, current density and polar plate surface area) and the operating parameters of the TEG they used in their study (i.e. the figure of merit ZT and thermal conductivity K) can have significant effects on the performance of this hybrid system.

Similar arrangement has been experimentally investigated by Hasani et al. [41] who performed waste heat recovery from a 5-kW PEMFC by using 4 thermoelectric coolers (TECs) for electricity generation. They found that the hot side of the TECs absorbed only about 10% of the total ~8 kW heat removed from the PFMFC stack. The energy conversion efficiency of the TECs was measured to be around 0.35% when the fuel cell stack operates at 68 °C. Very low efficiency of the TECs obtained in their experiment could be due to the fact that the TEC was restricted by low ionic conductivity of used semi-conduction materials at low temperature (< 100 °C) [196]. Deng at al. [90] tested the performance improvement of a 150-kW PEMFC (i.e. used in a tram) achieved by recovering its waste heat to generate additional power using TEGs. They found that at maximum power point of the stack, the TEGs could only generate about 1 kW of electricity, accounting for about 0.65% of total cooling load of the stack. The remaining heat (~99% that is almost close to its total) had to be still rejected from the coolant passing through a radiator to meet the cooling requirements of the stack. Recently, Kwan et al. [187] optimised the design of a TEG arrangement for PEMFC heat recovery application based on the NSGA-II genetic algorithm approach. They highlighted the importance of considering the existing trade-off between the maximum electricity generation of TEGs (i.e. the maximum system efficiency) and the total mass of the system. For example, when the mass of TEGs increases from 1.2 kg to 6 kg their power generation capacity increased from 2.2 W to 5 W.

Due to low operating temperature of LT-PEMFC, the electrical efficiency of TEGs used to recover their heat is very low (under 1%). On the other hand, with operating temperatures in the range of 120–200 °C (i.e. for HT-PEMFCs) the use of TEG for PEMFC heat recovery offers significantly-improved efficiency for the TEG modules (i.e. from under 1% to 3.5%) [186]. For example, by integrating the TEG modules with ZT = 1.1 in the cooling stream of 1-kW HT-PEMFC, Gao et al. [189] concluded that the theoretical energy conversion efficiency of the cell stack increased by 9.6%. The results showed that TEG heat recovery could generate maximum of 23 W of electricity that was equivalent to approximately 10% of the energy supplied by the Li-ion battery used in the system for fuel cell start-up. In another study, Gao et al. [197] developed a numerical model of a TEG with compact plate-fined heat exchanger for waste heat recovery from an open-cathode HT-PEMFC stack. An optimum system configuration for the TEG heat recovery system was then proposed after conducting a sensitivity analysis on key operating parameters such as temperature, mass flow rate and heat capacity of the cathode exhaust air. As part of their research and in a separate study, Gao et al. [186] tried to optimise their TEG heat recovery configuration for the HT-PEMFC stack. They reported that by optimising the electrical connection style of the TEG assembly, the power output of the heat recovery subsystem could increase by 40.6% compared to the results obtained in their previous studies: [189] and [197]. It was also found that if the ZT of commercial TEG modules increases from 0.5 to 2, the performance of HT-PEMFC heat recovery arrangement (i.e. using TEG) can increase from around 3.5% to over 10%.

5.3. Thermally regenerative electrochemical cycles

Utilising thermoelectric devices for electricity generation from PEMFC waste heat is limited by low ZT and low-temperature difference across TEGs. That is though the motivation to find alternative efficient methods for converting the low-grade heat collected from fuel cell into electricity. Thermally regenerative electrochemical cycles (TRECs) that work based on the temperature dependence of cell voltage of electrochemical systems to construct a thermodynamic cycle, is one of the alternative solutions for converting low-grade thermal energy into electricity [196,198,199].

The working principle of a TREC includes four steps: heating, charging, cooling and discharging (Fig. 16a). The system can generate power by discharging it at low temperature with high voltage and recharging at high temperature with low voltage (Fig. 16b). Because the TREC works as a heat engine cycle, it can be presented in the form of a thermodynamic cycle (Fig. 16**c**). During the heating process, the cell is heated from discharged state at low temperature (T_L) to high-temperature state (T_H) under open circuit voltage. Then, the cell is charged at a low voltage which requires heat absorption to increase the entropy of the cell during electrochemical reaction. During the cooling step, the cell is cooled down from T_H to T_L resulting in an increase in open circuit voltage. Finally, the cell releases heat to environment at T_L and is discharged at a high voltage. The work is extracted from this cycle due to the difference between charging and discharging voltage.

The maximum power generation by a TREC is the difference

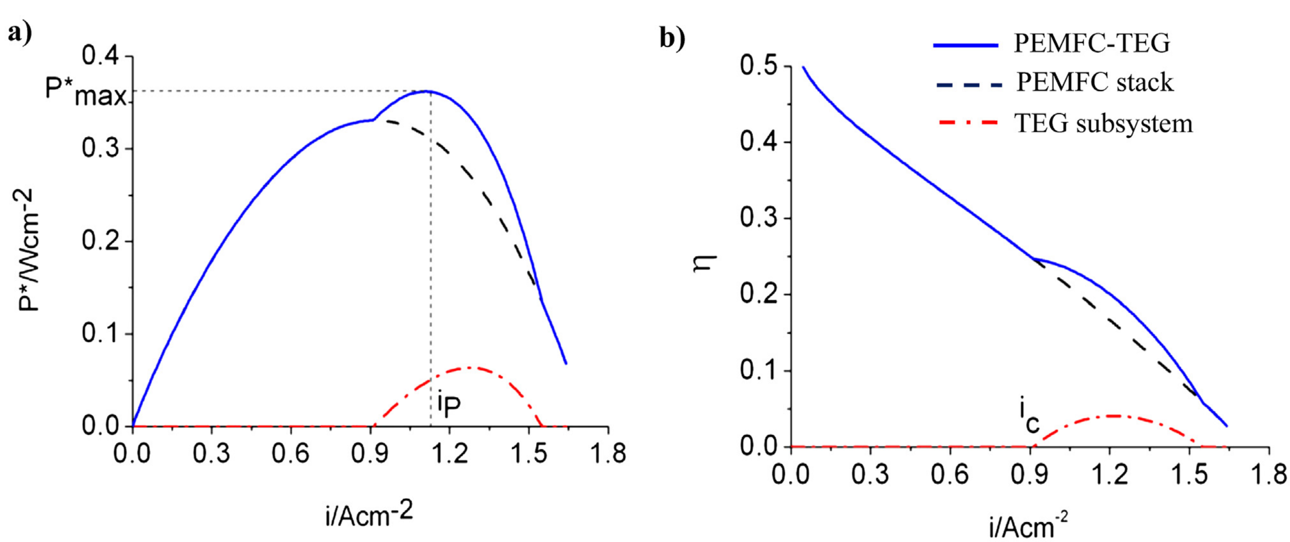

Fig. 15. Impacts of current density of PEMFC on: a) the total power density generation; b) overall energy efficiency of whole system [18].

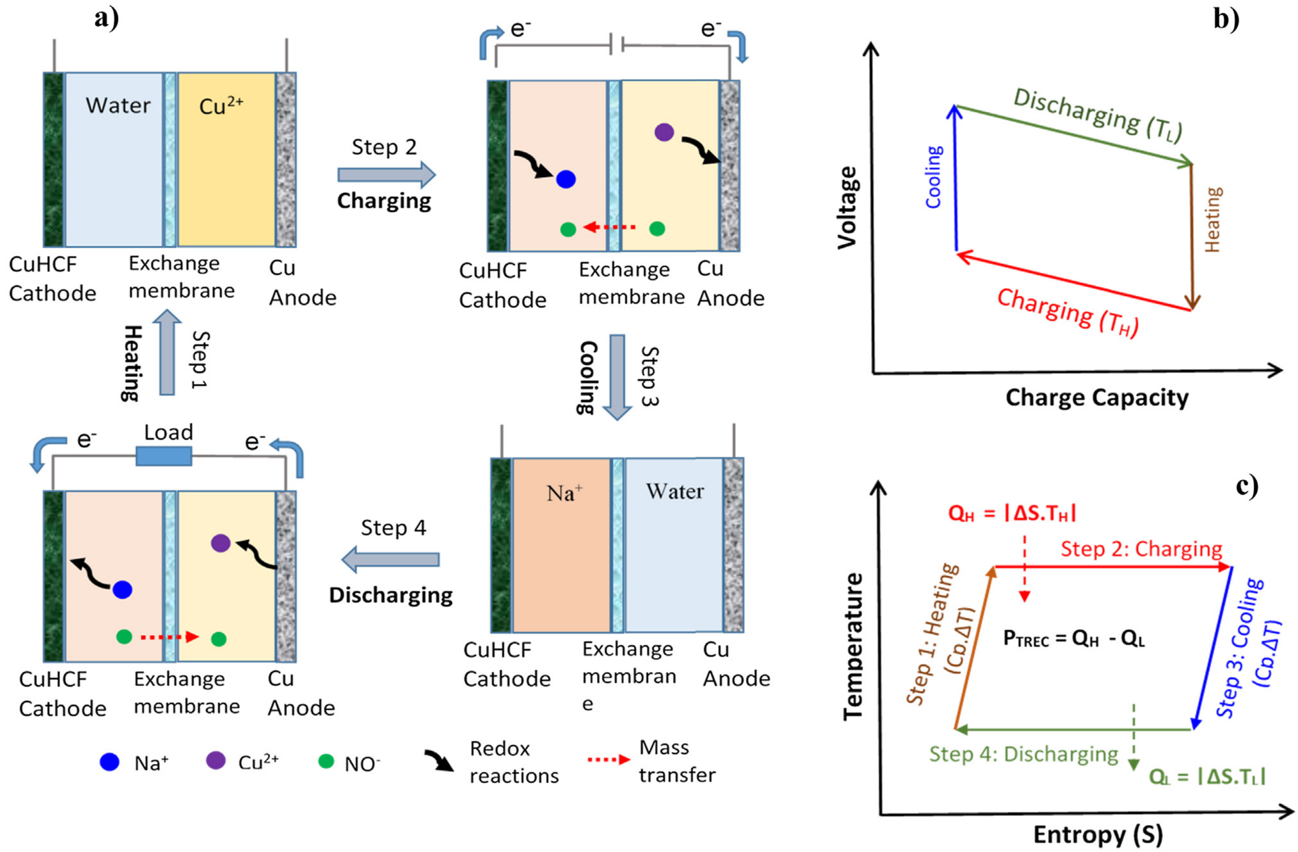

Fig. 16. Schematic diagrams of TREC for thermal energy harvesting [196,198,200]; (a) a TREC with CuHCF cathode and Cu anode with anion exchange membrane; (b) Voltage-capacity plot of a TREC; c) T-S diagram of a TREC.

between heat absorption rate ($\dot{Q}_H = T_H\Delta S$) at high temperature T_H and the heat release rate at ($\dot{Q}_L = T_C\Delta S$) low temperature at T_C. However, in practice, ohmic energy loss ($\dot{Q}_{TREC-loss}$) during charging and discharging of the TREC cell is expected that should be taken into account when calculating the real net power generation (P_{TREC}) of a TREC [201]:

$$P_{TREC} = \dot{Q}_H - \dot{Q}_C - \dot{Q}_{TREC-loss} = \Delta S(T_H - T_L) - I(R_H + R_L)nF \tag{15}$$

The energy conversion efficiency of a TREC (η_{TREC}) is the ration of the power generation and the total heat required for charging process. The thermal energy required for charging includes the heat required for heating up the cell ($Q_{heating}$) and heat absorption (Q_H). Hence, the energy efficiency of TREC can be expressed as [196,202]:

$$\eta_{TREC} = \frac{P_{TREC}}{\dot{Q}_H + \dot{Q}_{heating}} = \frac{\Delta S(T_H - T_L) - I(R_H + R_L)nF}{T_H\Delta S + \dot{Q}_{heating}} \tag{16}$$

In these equations, R_H and R_L are cell internal resistance at T_H and T_L; n is the number electron transfer of the redox reaction; F is the Faraday constant (96485 C/mol); ΔS is entropy change in the cell reaction of a TREC, and it can be calculated based on the temperature coefficient (φ_{cell}) of reversible electrochemical reaction in TREC as follows [198,202]:

$$\varphi_{cell} = \frac{\Delta S}{nF} \tag{17}$$

The TREC technology exhibited a 40–50% Carnot efficiency limit for high-temperature heat sources applications (i.e. 500–1500 °C) for few decades since 1960s [196,203]. However, most recently significant advancements were reported for reversible electrode materials allowing them to operate efficiently at lower temperatures [200,204–206]. This though suggested the technology to be a possible method for harvesting

Table 6
TREC for low-grade heat source energy harvesting.

Electrode pair	Heat source temperature (°C)	Heat recuperation (%)	Efficiency (%)	ZT equivalent	Reference
CuHCF,Cu/Cu^{2+}	10–70	0	3.7	1.8	[196]
		50	5.7	3.5	
$Fe(CN)_6^{3-/4-}$, Prussian Blue	20–60	70	2	0.9	[206]
NiHCF, Ag/AgCl	15–55	0	1.6	–	[198]
		50	2.6	1.4	
		70	3.5	2.1	
CoHCFe-pp, Prussian Blue	10–50	0	2.65	1.6	[202]
		50	3.65	2.6	
		70	4.31	3.7	
Cu/Cu^{2+}, $Cu/Cu(NH_3)_4^{2+}$	25–70	–	0.86	–	[208]
CoHCF, helical carbon nanotubes	20–70	0	1.18	–	[209]
			1.9	–	
			2.52	–	

energy from low-grade heat sources such as PEMFCs.

Lee et al. [196] innovated an electrochemical system using a solid CuHCF cathode and Cu/Cu^{2+} anode for efficient harvesting of low-grade heat energy. The thermal to electrical efficiency of 5.7% was reported for temperatures varying between 10 °C and 70 °C with 50% heat recuperation. As a comparison, for the same range of heat source temperature and temperature difference between heat source and sink, a TEG needs thermoelectric materials with ZT of 3.5 to operate at the same level of efficiency [196]. Similarly, by using electrodes $Fe(CN)_6^{3-/4-}$ and Prussian blue particles, Yang et al. [206] reported an energy conversion energy efficiency of 2.0% for a TREC operating between 20 °C and 60 °C. In another study, heat to electricity conversion efficiency of 3.5% was reported by Yuan et al. [198] when membrane-free TREC was discharged at 15 °C and charged at 55 °C, assuming heat recovery of 50% and 70%. Long et al. [207] conducted a multi-objective optimisation analysis on a TREC system for different low-temperature heat sources by considering maximum power output and exergy efficiency as the key objective functions. Table 6 summarises what reported in the literature on the performance of TREC technology in low-grade heat recovery for electricity generation.

Considering the operating temperature range of LT-PEMFC stacks TREC systems can be a promising option for recovering their heat for electricity generation. This solution has been investigated recently through several research studies. Long et al. [210] proposed a TREC system to convert the waste heat recovered from a PEMFC stack into electricity (Fig. 17**a**). In this configuration, the heat released from cooling process of the TREC (step 3) is recovered for the heating process (step 1) by a regenerator in order to improve the efficiency of the TREC subsystem. The results indicated that integration of TREC can increase the power output of the fuel cell system by 6.85–20.59% (Fig. 17**b**). Furthermore, they also pointed out that at the maximum power point of the fuel cell stack, by increasing the operating temperature from 70 °C to 95 °C, the electrical efficiency of the TREC subsystem increased from 4.56% to 13.8%, corresponding to 2.74% and 8.27% improvement in total electrical energy efficiency of the system at 70 °C and 95 °C respectively (Fig. 17**c**).

A single TREC cell is unable to absorb heat from the heat source continuously during the cycle period [211], thus causes the discontinuity of power generation [196,207]. Hence, as suggested and practiced by Zhang et al. [212], several TREC cells are to be utilised for the purpose of effective recovery of fuel cell heat and its conversion into electricity. Through their research, they showed that the output power of the fuel cell system enhanced by up to 20% by utilising multiple TRECs with efficiencies in the range of 0.2–0.8.

6. Thermal self-servicing of fuel cell systems

The heat from PEMFC systems can be used for keeping the temperature and hydrogen discharge rate of MH hydrogen storage systems, and for preheating the inlet reactants to improve the overall energy efficiency of the fuel cell stack.

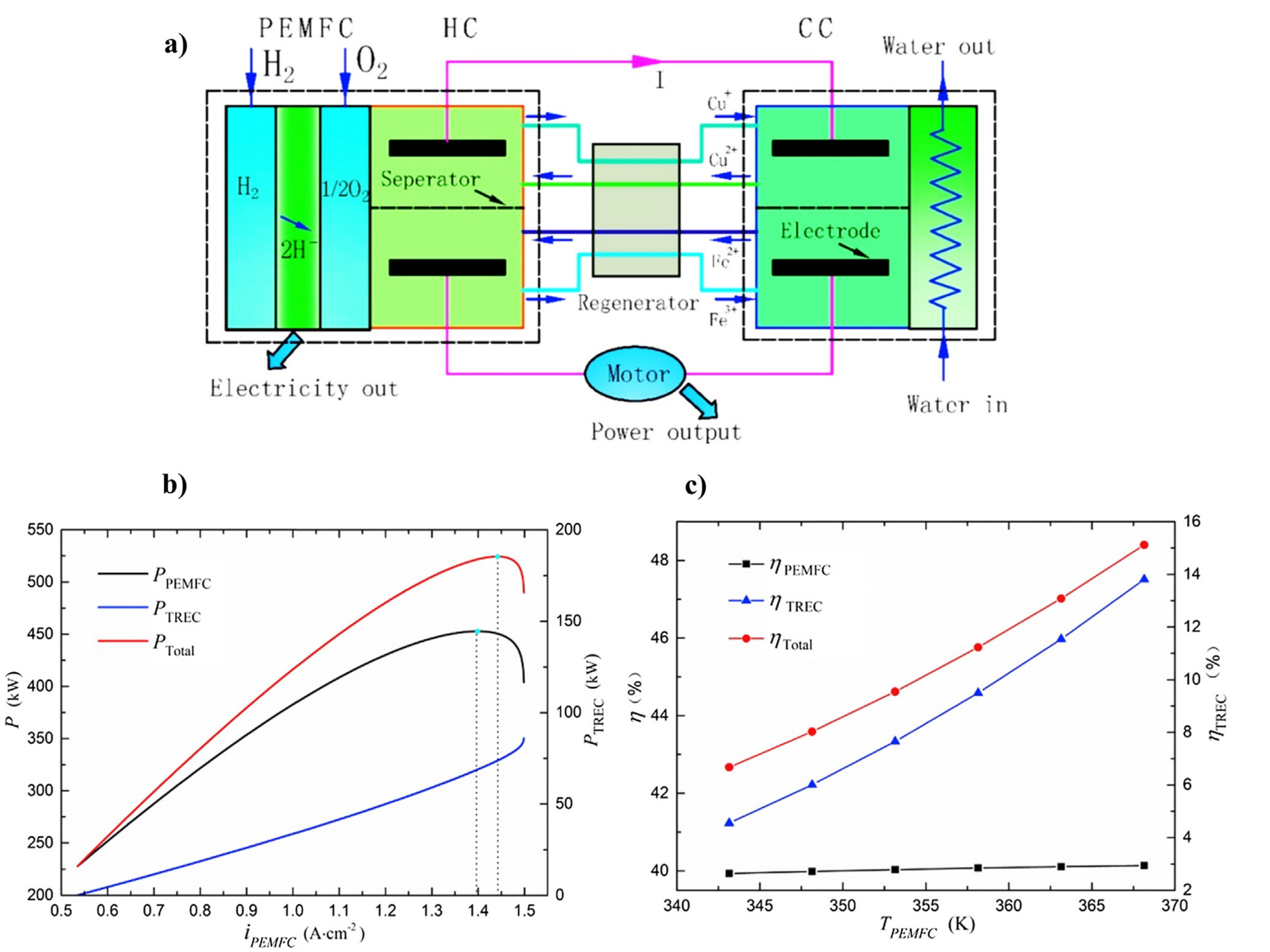

Fig. 17. a) Schematic diagram of the hybrid TREC with PEMFC systems; b) the impacts of current density on the power generation of PEMFC stack, TREC, and hybrid system; c) the impacts of fuel cell temperature on the energy efficiency of system [210].

Table 7
Summary studies of thermal coupling of MH and PEMFC.

Fuel Cell	Heating agent temperature	MH material type	Enhancing Heat transfer techniques	Thermal coupling approach	Ref
1.2 kW LT-PEMFC, air cooling	39 °C	AB2 alloy	External Aluminium Fins or internal annular	Direct hot air cooling	[222]
0.2 kW LT-PEMFC, air cooling	NA	90% AB2 + 10% AB5 alloy	External Fins + internal Thermal Expanded Graphite	Direct hot air cooling	[223]
0.3 kW LT-PEMFC, air cooling	NA	Ovonic (85G555B-NPT)	NA	Direct hot air cooling	[224]
LT-PEMFC, air cooling	50–55 °C	AB5 alloy	NA	Direct hot air cooling	[220]
2.5 kW LT-PEMFC, air cooling	40–50 °C	AB5 alloy	NA	Direct hot air cooling	[218]
5 kW LT-PEMFC, air cooling	40–48 °C	Ovonic (OV679)	Internal water tubes	Direct hot water (capture heat from hot air via heat exchanger)	[225]
6 kW LT-PEMFC, water cooling	50 °C	AB5 Alloy	External hot water tube coils holder	Direct hot water cooling	[226]
80 kW LT-PEMFC, water cooling	65 °C	Sodium alanate	Internal water tubes	Direct hot water cooling	[227]
1.2 kW LT-PEMFC, water cooling	60 °C	AB5 alloy (LaNi4.8Al0.2)	External jacket + Copper fins	Indirect hot water (via heat exchanger)	[228]
LT-PEMFC, water cooling	NA	AB2 alloy	Expanded Natural Graphite + Water bath	Indirect hot water (via radiator)	[229,230]
5 kW LT-PEMFC, cooling water	50–70 °C	AB5 alloy (LaNi5)	Internal tubes assisted metal foam	Direct hot water cooling	[144]
1.2 kW LT-PEMFC, water cooling	30–50 °C	AB5 alloy (Ce modified LaNi5)	Internal U shape tube assisted copper fins	Direct hot water cooling	[219]
1 kW HT-PEMFC, cathode air cooling	130 °C	Sodium alanate (NaAlH4)	Heat jacket	Direct hot air cooling	[231]
0.4 kW HT-PEMFC, organic liquid	160 °C	sodium alanate (NaAlH4)	External copper tube coils	Direct liquid cooling	[232]
0.26 kW HT-PEMFC, thermal oil cooling	120–150 °C	Sodium alanate (NaAlH4)	Internal tube coil	Direct liquid cooling	[221]
1.2 kW HT-PEMFC, thermal fluid cooling	120–160 °C	(LiNH2/MgH2)	Heat jacket	Direct liquid cooling	[233]
0.4 kW HT-PEMFC, thermal oil	160–185 °C	Sodium alanate doped Ce	Heat jacket	Direct liquid cooling	[234]

6.1. Thermal coupling with metal hydride hydrogen storage canisters

High volumetric hydrogen storage capacity (i.e. ~100 g/L), stability, low storage pressure (i.e. usually less than 20–30 bar), high purity of supplied hydrogen, and reversibility (hydrogen charging and discharging processes) make metal hydride (MH) a promising solution for storing hydrogen [213]. Metal hydride is formed by reversible reaction at moderate temperatures and pressures with a substantial amount of enthalpy change. Hydrogen desorption in MHs is an endothermic process that requires heat to maintain its temperature at a required level (usually in the range of 20–30 °C) for releasing hydrogen at a stable rate. Depending on plateau pressure, temperature and MH's material, the magnitude of required heat (enthalpy change) for hydrogen desorption varies in the range from 10 to 20% of hydrogen's HHV [213].

The hydrogen desorption rate from a MH hydrogen storage system is based on the reaction kinetics that is expressed as the hydrogen mass desorbed per unit time and unit volume ($\dot{m}_{MH}$) and can be obtained using the following equation [214,215]:

$$\dot{m}_{MH} = C_d.\ \exp\left(\frac{E_d}{RT}\right)\left(\frac{P - P_{eq}}{P_{eq}}\right)\rho_s \tag{18}$$

where C_d is the desorption constant (1/s); E_d is the activation energy of desorption process, (J/mol); P_{eq} is equilibrium pressure, (N/m^2); T is absolute temperature of MH tank, (K); R is the universal gas constant (8.314 J/mol.K); and ρ_s is the density of metal hydride (g/m^3).

The equilibrium pressure of MH is a function of absolute temperature as shown in the Van't Hoff equation below [216–218]:

$$P_{eq} = \frac{\Delta H}{RT} - \frac{\Delta S}{R} \tag{19}$$

where ΔH is the enthalpy change of metal hydride, (J/mol); and ΔS is entropy change, (J/molK).

From Eqs. (18) and (19), it can be seen that the reaction kinetic of the hydrogen desorption in the MH bed is closely linked to its temperature. Due to endothermic process of the hydrogen discharging, heat at a specific rate ($\dot{Q}_{MH}$) must be supplied to the MH canister to keep its temperature at a desired level and hence to maintain its hydrogen release rate ($\dot{m}_{MH-H2}$). The amount of this heat is calculated using the following equation [42,219]:

$$\dot{Q}_{MH} = \dot{m}_{MH-H2}.\ \Delta H \tag{20}$$

where $\dot{Q}_{MH}$ is the heat rate required by MH canister during desorption, (W); $\dot{m}_{MH-H2}$ is hydrogen release rate from MH, (mol/s). During the steady-state, the hydrogen release rate can be calculated by equation:

$$\dot{m}_{MH-H2} = \frac{\dot{m}_{MH}.\ V_{MH}}{M_{H2}} \tag{21}$$

where V_{MH} is the volume of MH tanks, (m^3); M_{H2} is the molar mass of hydrogen, (g/mol)

The technical challenge of matching the hydrogen capacity in MH tanks with the maximum hydrogen rate required by a PEM fuel cell stack (i.e. particularly at high power generation rates), is usually solved by oversizing the hydrogen storage capacity and/or introducing an external heat source to increase the temperature of MH tanks and hence enhance their hydrogen discharge rate. While these solutions cause unwanted increase in the capital costs and weight of the system, the latter results in an increase in the parasitic energy consumption, and thus reduces the overall energy efficiency of the system. Consideration the significant amount of heat generated in a PEMFC (i.e. up to 60–70% of hydrogen's HHV) at around 60–80 °C (i.e. in a LT-PEMFC), its thermal coupling with MH canisters is an attractive solution to enhance the performance of the system. This can help reduce the parasitic energy of the system while helping with particle removal of the heat generated by the fuel cell. Such an idea has been practiced before in the form of both active and passive arrangements as reported in the literature [43,219–221].

In active thermal coupling techniques, the coolants (air or liquid) are used to transfer the fuel cell heat to MH canisters during the desorption process. Several studies have been conducted to date on the feasibility and performance of such thermal coupling arrangements. Table 7 summarises the specifications and the equipment used in some of key recent case studies on the active thermal coupling of PEMFCs and MH hydrogen storage systems.

The cooling strategy used for the stack can influence the configuration selected for thermal coupling between MH canisters and the fuel cell. For example, in an air-cooled PEMFC stack, the MH canisters can be directly warmed up using the hot cooling air stream flowing cross over the external surface of canisters (the canisters can be finned on their external surface) [220,222–224]. A typical schematic diagram of thermal coupling of an air-cooled PEMFC and a MH canister is shown in the Fig. 18. As detailed in this figure, Davids et al. [223] developed a portable air-cooled PEMFC fuelled by a mixture of AB2 and AB5 alloy MH canisters mounting where the coolant (air) exits the stack to capture the fuel cell heat removed from the fuel cell. The results showed that by reusing the PEMFC heat for heating up the MH canister, it was able to supply a stable rate of hydrogen to the fuel cell for over 40 min.

With the help of a similar arrangement as that illustrated in Fig. 18, an Ovonic MH canister with 68 g hydrogen storage capacity, could provide a stable supply of hydrogen at a rate required for a 0.3 kW used to run a little 25-liter freezer for 7 h [224]. Borzenko and Eronin [220] experimentally investigated the feasibility of utilising hot air coolant from a 1.1 kW and a 2.5 kW PEMFC to assist the hydrogen desorption process in a 800 NL metal hydride hydrogen storage system. The results indicated that the MH reactor, which was thermally treated using an air-liquid heat exchanger, could provide a steady flow of hydrogen to the 1.1 kW PEMFC for more than 1 h. However, it failed in meeting the hydrogen flow rate required for the 2.5 kW PEMFC. This indicated that improvement in the discharge rate of hydrogen from a MH using the heat supplied by the fuel cell could face a limit.

Omrani et al. [218] developed a mathematical model to simulate the heat transfer between a 2.5 kW open-cathode PEMFC exhaust heat and MH canisters, followed by an experimental work to confirm their findings. The results of this study showed that without thermal coupling with the fuel cell stack, a considerable number of MH canisters are required (e.g. 31 MH canisters of 800-sl storage capacity for continuous operation at 2 kW power output, at 20 °C of ambient temperature). However, the quantity of MH canisters required reduces by around up to 70% when the exhaust hot air from the fuel cell was supplied over the MH canisters.

The heat extracted from HT-PEMFC operating at 120–200 °C has also been utilised for maintaining the temperature of MH tanks during discharging process [44,231]. As provided in Table 7, solid hydrogen storage based intermetallic hydrides (i.e. AB2 and AB5) is more suitable for thermal coupling with LT-PEMFC because they demonstrate an equilibrium pressure above atmospheric at temperature range from 20 °C to 80 °C. However, the main disadvantage of these types of MH is low gravimetric hydrogen capacities (1.5–2 wt%) [213]. Sodium alanates-based MHs (i.e. $NaAlH_4$ and Na_3AlH_6), which have theoretical gravimetric hydrogen storage capacities of 5.5–7.4 wt% and desorption temperature of 90–165 °C at 10 bar plateau pressure to release the whole hydrogen content [213,235], can best benefit out of thermal coupling with HT-PEMFCs. The possibility of thermal coupling between HT-PEMFC and sodium alanates has been experimentally and theoretically investigated by several researchers [221,232,234]. The results showed that the heat captured from a HT-PEMFC stack can significantly enhance the hydrogen release rate of high capacity MH canisters and eliminate the need for utilising an external source of heat for this purpose. [221]. Reddy and Jayanti [44] investigated the possibility of using cathode air to cool a 1-kW HT-PEMFC stack and supply the heat required for hydrogen discharging of a sodium alanate MH storage system. They found that waste heat from cathode air flow at stoichiometry of 7 is enough for both preheating the inlet cathode air (this will be further discussed in next Section 6.2) and thermal management of the MH used in their study.

Similarly, the results obtained by Yiotis et al. [231] indicated that heat flux from cathode air stream at air stoichiometric of 12 and temperature of 130 °C is theoretically sufficient for maintaining the hydrogen release rate (from a MH) required to meet the demand of a 1 kW HT-PEMFC at moderate power outputs. However, despite the high temperature of exhaust air (130 °C), the hydrogen release rate was not sufficient to keep the fuel cell operation close to its rated power (e.g. at 0.8 kW or 1 kW) due to low thermal conductivity (using external heat

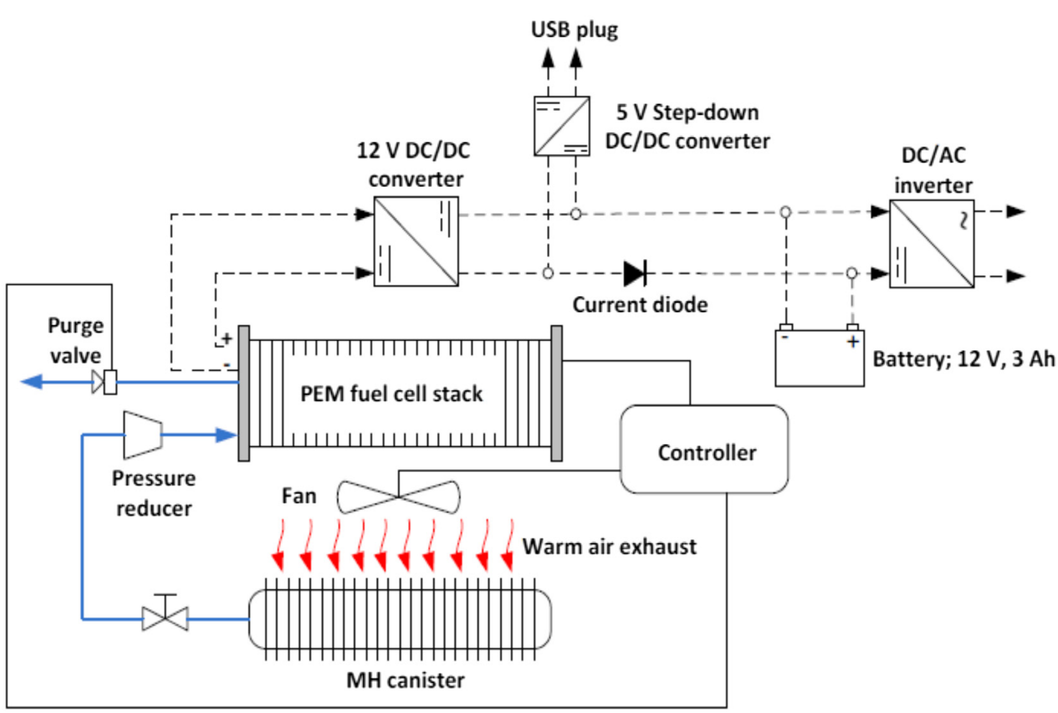

Fig. 18. The schematic diagram of thermal coupling of an air-cooled PEMFC with a MH canister used by Davids et al. [223].

jacket without fins) of MH tank. It is important to note that because air coolant is characterised as a medium with a very low thermal conductivity, heat transfer enhancement techniques such as using fins on the air side, for MH tanks are needed to improve the hydrogen desorption rate and maintain this for extended periods. In fact, several studies showed that without applying such heat transfer enhancement techniques, the MH may fail to supply the required hydrogen flow rate for fuel cell, particularly over extended periods, and especially at high power outputs [222,231].

A common heat transfer enhancement technique is increasing the heat transfer area by introducing high thermal conductivity metal fins (i.e. aluminium and copper fins) on the outer surface of MH canisters. One of the key attractions of MH hydrogen storage solutions is their relatively high volumetric hydrogen storage capacity in comparison with other solutions such as high-pressure gas and cryogenic options. However, this advantage is obviously diminished by adding external fins as it adds significantly to the overall volume occupied MH canisters. This also adds to the already high mass of this solution. Some other configurations for capturing heat from air-cooled fuel cells for thermal management of MH canisters have been introduced that they all similarly contributes additional volume and mass to the system, while some of them may arguably make the overall thermal management/coupling arrangement complex [213,236].

It is noteworthy that condensation of water vapour in the air coolant (i.e. mostly picked from the fuel cell) on the fins and MH surface should be taken into account. The relative humidity of the exit air stream is usually close 100% that makes the water condensation highly likely when the temperature of fins and canisters fall below the dew-point temperature of this exit air stream (due to endothermic process in MH) [220,237]. This then can help with water recovery from the fuel cell system as an attractive solution in some applications.

From the performance point of view, introducing air-to-liquid heat exchangers offered some promising performance indicators. Example of this is the air-to-liquid heat exchanger used by Song et al. [225] for thermal coupling of a 5-kW of an air-cooled PEMFC with 4 AB2 MH tanks, capable of storing 3 kg of hydrogen. It should be mentioned that this arrangement needs a pump to circulate the liquid suggesting a new source of parasitic energy. Khayrullina et al. [238] developed a prototype of 1 kW air-cooled PEMFC and a 1000 l of $LaNi_5$ MH reactor using waste heat utilisation from fuel cell stack to replace external heat for hydrogen desorption process. A radiator was used to capture heat from hot air for the hot water circulation in MH reactor. The outcomes of their studies showed that the fuel cell stack is unable to keep operating when starting from high power loads (i.e. greater than 500 W), because the heat delivered by the coolant is not enough to heat the MH reactor.

Implementing options for the fuel cells that are already liquid-cooled seems to be more practical with less additional implications. Typical schematic diagram of thermal coupling of a liquid-cooled PEMFC and a MH canister is shown in Fig. 19. Førde et al. [219] analysed the enhancement of the hydrogen release rate of a 17.5-kg AB5 metal hydride canister, with storage capacity of 2.9 Nm^3 hydrogen, used to supply hydrogen to a 1.2-kW PEMFC by recovering waste heat through a U-tube heat exchanger embedded into the MH canister. The results indicated that by capturing 25% of total cooling load of the PEMFC, MH canister matches hydrogen demand for 3 h of stack's operation at the maximum power point. This is while the system initially failed to operate without this thermal coupling arrangement. A number of other researchers, who studied the possibility of thermal coupling arrangement between the fuel cell and MH canisters, also reported that 20–30% of the fuel cell cooling load is sufficient to enhance the hydrogen release rate of the MH canisters to the level required for proving a continuous supply of hydrogen to the fuel cell [42,67,227]. This shows that an additional cooling arrangement is still required to remove the remaining cooling load of the fuel cell.

The small temperature gap between the fuel cell coolant (particularly in LT-PEMFCs) and the ambient can be a challenge for cooling in applications with space restrictions, as this suggests for larger size radiators to be used to maintain the required flow of heat removal from the fuel cell [92,94]. Hence, circulating the coolant throughout the MH hydrogen storage unit and then directing it towards the heat exchangers can exacerbate the above-mentioned challenge. That is why alternative configurations such as devising parallel thermal management circuits for the MH canisters and the fuel cell heat exchanger can be taken into consideration [228].

The design of the heat exchanger integrated into the MH canisters plays a vital role in capturing the waste heat from the fuel cell stack. From the heat transfer point of view, due to higher heat transfer coefficient and better direct contact between MH alloy and the cooling media, a water-based heat exchanger embedded into the MH tanks can be more compact than air-based ones with external fins. As can be seen in Table 7, several types of heat exchangers, such as those with internal tubes, U-shape tubes, heat jacket, and external coils, have been developed to date and integrated into MH hydrogen storage unit as part of thermal coupling arrangement between liquid-cooled PEMFCs and the MH canisters. The metal alloy powder beds exhibit very poor thermal conductivity (i.e. as low as ~0.1 $Wm^{-1}K^{-1}$) [239–241] that makes the heat transfer throughout the MH a challenging task. It has though been suggested that as a reasonable technical target for metal hydride canisters, the effective thermal conductivity of the metal bed should be greater than 8.4 $Wm^{-1}K^{-1}$ [242]. Therefore, various thermal conductivity enhancement techniques (i.e. for metal power bed in the MH), such as inserting fins, using metal foam materials, and micro-encapsulated metal hydride compact, have been proposed. Example of inserting internal fins for improvement of heat transfer rate in MH bed is shown in Fig. 20.

It is important to keep in mind that adding such materials for enhancing heat transfer reduces the volumetric hydrogen storage density. More details of heat transfer techniques in the MH tanks for thermal coupling applications can be found in reference [236].

As already discussed in the Section 2, passive cooling using heat pipes with high effective thermal conductivity allows for eliminating parts such as fans, pumps, pipes and radiator that are normally used in active cooling systems. This then reduces the total mass, volume, complexity, and parasitic energy of the fuel cell system while enhancing its reliability [43,59,60]. However, research on passive thermal coupling between PEMFC and MH storage tanks has only been studied limitedly. Heat pipes have though been suggested for passive thermal bridging of PEMFCs and MH canisters. A novel model of thermal coupling of a 500-W PEMFC and MH hydrogen canisters using heat pipe was developed by Tetuko et al. [42]. In this model, the evaporator sections of the heat pipes were integrated into the cooling plates of the fuel cell to remove the heat generated in the cells and transfer this heat to metal hydride canisters (i.e. connected to the condenser sides of the

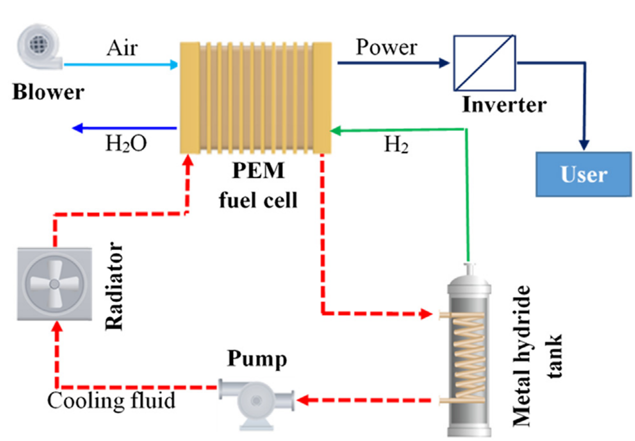

Fig. 19. Typical schematic diagram of thermal coupling of liquid-cooled PEMFC and MH tank.

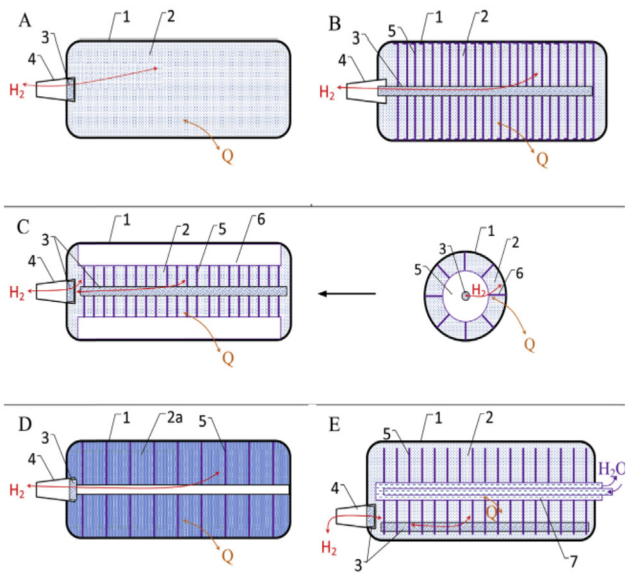

Fig. 20. Heat transfer enhancement techniques for thermal coupling MH and PEMFC: A – simplest layout; B – added internal fins; C – comprised longitudinal fins; D – MH/TEG compact assisted by fins; E – internal heat exchanger assisted by fins [229].

heat pipes) (Fig. 21**a**). The results showed that the five canisters (storing 69 g of hydrogen each) used in this study required about 20% of the total heat generated by the fuel cell to maintain the flow of hydrogen at 7.2 slpm required by the fuel cell to operate at 500 W. In another research published by Tetuko et al. [67] they conducted an experimental study on this concept using a MH canister (~80 gr H_2 capacity) and a 4-cell PEM fuel cell equipped with one cooling plate operating at 130 W (Fig. 21**b**). This study validated the outcomes suggested by their earlier theoretical modelling.

The experimental results obtained by Tetuko et al. [67] showed that without thermal coupling of MH canister and the fuel cell stack, the temperature and hydrogen discharge rate of the MH decrease after 10–15 min resulting in a drop in the capacity of the stack in proving high power rates (Fig. 22**a**). Meanwhile, by capturing heat from the fuel cell stack using heat pipes, the average temperature of the outer surface of MH can increase up to 42 °C during 1400 s of operation (Fig. 22**b**). Consequently, the MH canister was able to continuously supply sufficient hydrogen rate (i.e. ~1.7 slpm) for stable and continuous operation of the fuel cell at 130 W.

Thermal coupling of PEMFC and MH using heat pipes helps reduce the size of the active cooling system required for the fuel cell as part of the heat is used by the MH canisters. This will though offset the additional mass required for thermal coupling purpose. Moreover, apart from free supply of energy required for thermal management of the MH canisters, this arrangement would also help reduce the parasitic energy involved in the cooling of the fuel cell (i.e. as a smaller cooling system is used).

6.2. Preheating (thermal conditioning) the reactants

Another application for the heat recovered from a PEMFC is preheating the reactants (i.e. inlet air and/or hydrogen) in particularly extreme cold climate conditions. Previous studies were mostly focused on highlighting the benefits of preheating the inlet air due to its close link with fuel cell water management [24,243]. For HT-PEMFCs, heat recovery for preheating the inlet cathode air can reduce the cold-start time and thermal stress that is due to significant temperature difference between cells (i.e.120–180 °C) and air reactant (e.g. below 25 °C). This will though improve the durability of fuel cell stacks operating in such conditions [244]. It is noteworthy that when a cell stack operates in sub-zero temperature environment, issues such as performance degradation, membrane dehydration, long-term durability impacts, and slow start-up caused by ice formation of water would be pronounced even more [24,245]. Using external heat sources (i.e. to preheat the inlet air) results in an increase in the parasitic energy consumption of the fuel cell system, and hence reduces its overall energy efficiency. A potential solution for this problem is utilising the waste heat from the PEMFC to preheat its own inlet air reactant.

By using air-to-air heat exchangers to recover the heat of a 2-kW open-cathode LT-PEMFC for preheating inlet air, Nguyen et al. [24] conducted a theoretical study on this possibility in the context of a fuel cell-based telecommunication system operating in extreme cold climate conditions (i.e. up to −40 °C). The results indicated that after passing the transition phase and operating the fuel cell at its ideal temperature

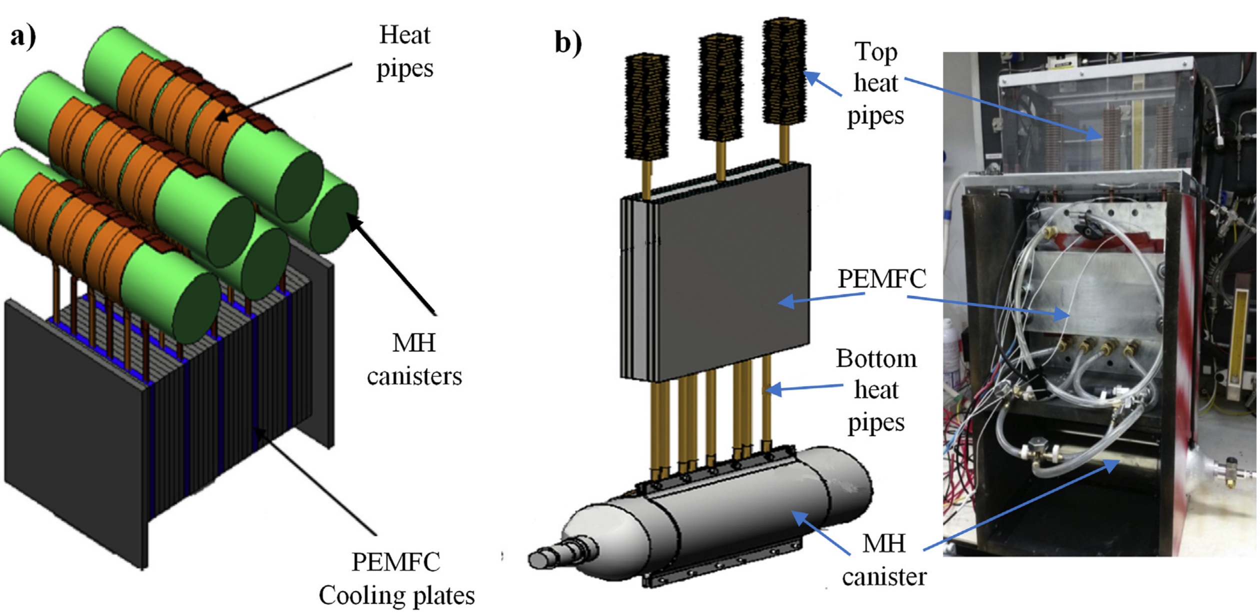

Fig. 21. a) Configuration of passive thermal coupling MH and PEMFC by heat pipe [42]; b) Experimental set-up of thermal coupling arrangement of 300 W PEMFC and 800 sl MH canister [67].

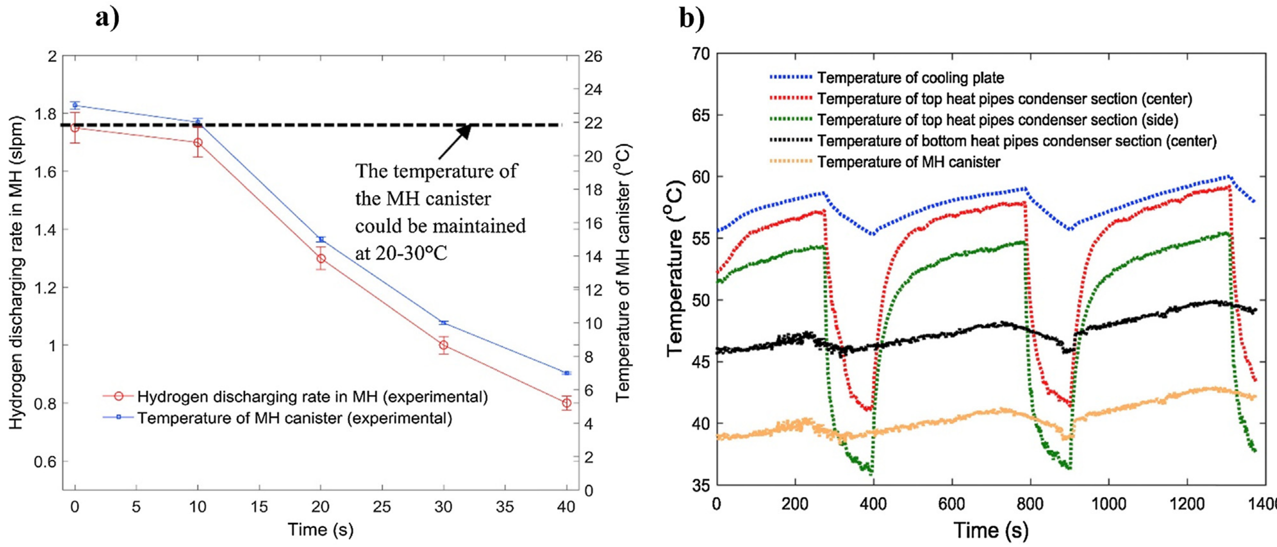

Fig. 22. a) Hydrogen discharge rate of MH canisters and its temperature profile over time without thermal coupling; b) Temperature variation of the key components (fuel cell cooling plates, heat pipes and MH) overtime with thermal coupling arrangement using heat pipe [67].

range (i.e. 65 °C) it was possible to push the air temperature from −40 °C to above 0 °C by recovering the heat generated by the fuel cell. The schematic diagram of their PEMFC and the heat recovery arrangement used for preheating its inlet air is presented in Fig. 23.

Nernst and Tafel equations indicate that operating a PEMFC at higher pressure and temperature lead to delivering power at better efficiencies (i.e. lowering the overpotentials) [15,246]:

$$E_{Nernst} = \frac{\Delta G^0}{2F} + \frac{RT}{2F} ln\left(\frac{P_{H2}.\ P_{O2}^{0.5}}{P_{H2O}}\right) \tag{22}$$

$$\Delta V_{act} = \frac{RT}{2\alpha F} ln\left(\frac{i}{i_O}\right) \tag{23}$$

In these equations, E_{Nernst} is Nernst potential (V); ΔG^0 is Gibbs free energy of reaction; F stands for Faraday constant (96485C/mole); R is universal gas constant (8.314 J/mole); T is the operation temperature of fuel cell, (K); P_{H2}, P_{O2}, and P_{H2O} are the supply hydrogen pressure, partial oxygen pressure, and water product pressure respectively; ΔV_{act} is activation overpotential (V); α is charge transfer coefficient; i_O is exchange current density (A/cm^2); and i is current density (A/cm^2).

From the Nernst equation (Eq. (22)), it can be found that the Nernst potential increases by increasing the operating temperature of the fuel cell. A faster reaction between hydrogen and oxygen occurs at higher operation temperature resulting in higher exchange current density. Therefore, increasing the temperature leads to a decrease in the activation overpotential.

From the thermodynamics point of view, increasing the temperature of an ideal gas (i.e. hydrogen) for a given mass flow rate would help increase the pressure. According to Nernst and Tafel equations, this will increase the open circuit voltage while decreasing the activation losses

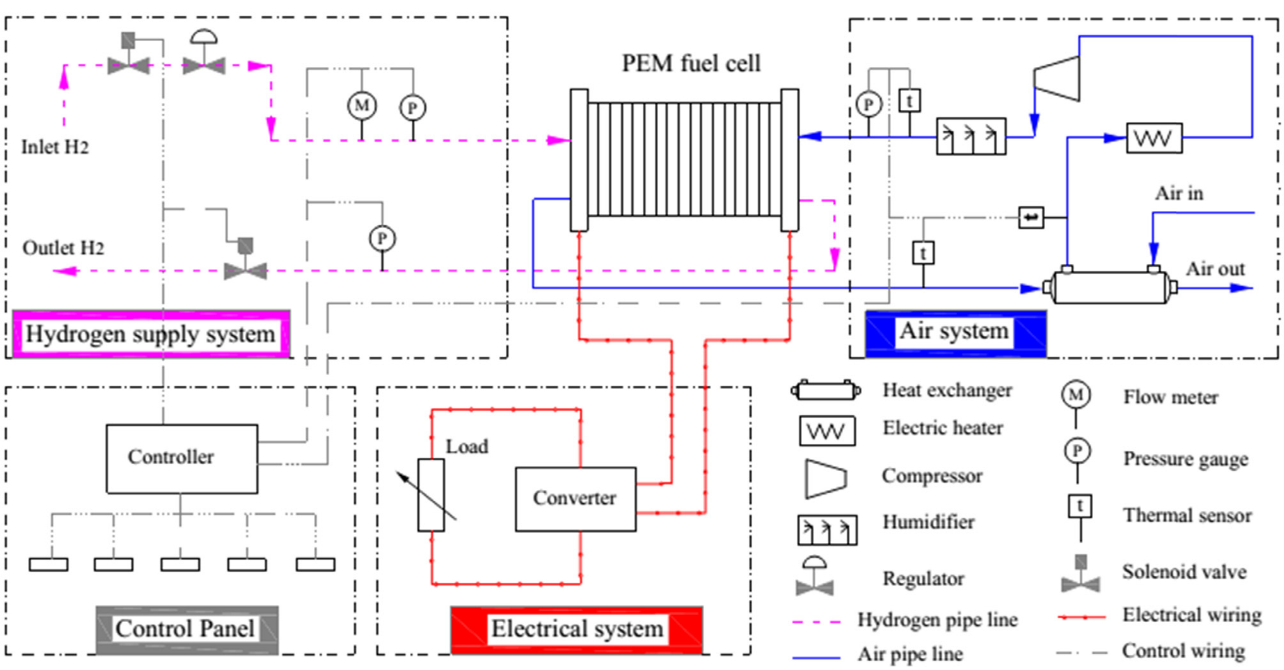

Fig. 23. Schematic of a PEMFC with heat recovery arrangement for preheating (thermal conditioning) the inlet air to be operated under extreme cold climate condition.

(i.e. higher power output). By taking this into account Mohamed and Kamil [45] experimentally investigated the opportunities for improving the performance of an open cathode PEMFC by capturing heat generated in the fuel cell for preheating the inlet hydrogen. The results of their study showed that depending on the stack power output, by using 3–6% of the heat generated by the fuel cell, the hydrogen temperature could be increased in the range of 2–13 °C, and consequently the stack power could be increased by up to 10%. Apparently, the rest of the fuel cell heat can still be recovered and used for other on-site thermal applications.

7. Opportunities for future research and development

A range of ideas has been presented and demonstrated around harvesting the heat generated by PEMFCs and utilising this heat for a range of applications. However, the broad literature review conducted to accomplish this study clearly indicates several areas to receive attention:

7.1. Dedicated economic assessment studies

The economic viability of PEMFC heat recovery systems has not received due attention in the literature. Even with some solutions the published studies have mainly remained limited to only proving the technical feasibility of the technological solutions being proposed. For example, capturing low-grade heat from PEMFC cell stacks to drive thermodynamic cycles such as absorption refrigeration cycles, organic Rankine cycle and regenerative electrochemical cycle has been proven to be technically feasible. However, there is not any paper published up to date investigating the economic performance of such power cogeneration solutions. A similar gap (lack of a dedicated economic assessment) can be seen in the literature focused on many other PEMFC heat recovery solutions such as those presented for using the fuel cell heat for thermal management of MH hydrogen storage systems.

7.2. System optimisation

Going one step further, optimisation studies on these heat recovery solutions and applications is another obvious gap in the literature. For example, very little has been done on multi-objective optimisations around sizing and operating of PEMFC heat recovery systems. It is well known that relatively high cost of PEMFC-CHP systems (e.g. compared to fossil fuel-based CHP systems), has remained to be one of the main drawbacks of wider implementation of these systems. Targeted system optimisation can help address the high capital and running costs of PEMFC CHP systems and support their economic viability.

7.3. Exergy analysis

It is important to note that in many cases exergy analysis can be a strong tool along with energy analysis to support optimisation studies on such systems. This can shed light from a different angle on opportunities for achieving better techno-economic performance of the system (i.e. helping with system optimisation). Despite this, the literature is presenting very little on exergy analysis of fuel cell heat recovery solutions indicating a clear research gap out there to be addressed.

7.4. Hybrid integrated renewable solutions for 100% heat and power supply

Most of the current PEMFC-CHP systems have been designed for meeting 100% of power demand of the application for which the systems are used for. Therefore, usually only part of the thermal demand of the application is met using the heat recovered from the fuel cell. Integrating the system with other (preferably renewable) solutions to also achieve 100% supply of heat is an important area to receive further attention, particularly for standalone applications. The studies conducted by Jihane et al. [152,158,159] are some of the limited ones dealing with such solutions. However, the literature is suggesting significant opportunities yet to be explored around such hybrid integrated solutions.

7.5. Possibilities for multiple thermal applications

The existing studies have all focused on only one application at a time for the heat released from a fuel cell. However, fuel cell heat can be utilised for more than one thermal application in some cases (where the opportunity is presented) that potentially helps improve the economic viability of the system. For example, when fuel cell heat is used for thermal management of MH systems, according to the literature, only ~20 to 30% of the total heat available from the fuel cell is required for this purpose; hence, the rest of the fuel cell cooling load can be considered for other on-site thermal applications. Furthermore, in the TEG based PEMFC heat recovery systems, the energy conversion from heat to power by TEG modules accounts for under 10%. The remaining of the fuel cell heat (greater than 90%) can be captured and utilised for other purposes, such as CHP applications [247] or preheating the inlet reactants to improve the performance of PEMFC stacks.

7.6. Fresh water production

With the increasing demand for fresh water, low-grade heat driven water treatment technologies (i.e. multi-effect distillation and direct contact membrane distillation) has been considered as an effective waster heat recovery method. The applications of renewable energy sources (i.e. solar thermal and geothermal) for fresh water production was widely studied and summarised by Ghaffour et al. [248] and Eltawil et al. [249]. The working temperature range of membrane distillation and multi-effect distillation is around 50–90 °C [248], which matches very well with the operating temperature range of PEMFCs. Up-to-date, only a study was done by Lai et al. [250], who investigated the use of direct contact membrane distillation to recover the heat from a PEMFC for bine water desalination. Therefore, more works on fuel cell heat recovery for fresh water production should be taken into consideration in the future.

8. Conclusions

The heat recovery opportunities from PEMFCs have been thoroughly reviewed in this review work. The heat generation mechanisms in the fuel cell stack, cooling strategies to keep their operation temperature in the desired range, as well as opportunities for recovering low-grade heat streams supplied by PEMFC was discussed. Despise the low quality of the heat recovered from a PEMFC (i.e. particularly low temperature PEMFCs), the amount of heat in the coolant stream is sufficient to be captured and utilised for a wide range of applications such as heating in CHP systems, cooling in CCP/CCHP systems, power generation systems, preheating the inlet reactants, and thermal managements of metal hydride canisters.

Heat recovery from the PEMFC systems for supplying both heat (e.g. hot water or space heating) and power purposes improves the overall energy efficiency of the fuel cell (i.e. from ~30 to 50% for power supply alone to ~70 to 90% for CHP applications), reduces operating costs, and the GHG emissions significantly. In renewable-hydrogen (e.g. solar-hydrogen) based PEMFC systems, heat recovery from the fuel cell stack helps improve the overall round-trip energy efficiency of the hydrogen-based energy storage system (up to about 50%), which allows this energy storage solution to be more competitive with batteries even in short-term energy storage applications. Because most of the PEMFC heat recovery systems can only partially meet the thermal demand of the applications, filling in this gap using other renewable energy technologies (i.e. solar thermal collector) should be considered to avoid the use of boosters running on fossils fuels.

The idea of capturing and reusing the heat from PEMFC to drive sorption refrigeration cycles for CCP/CCHP applications also offers opportunities to improve the overall energy efficiency of the PEMFC system. Adsorption cooling systems using solid-vapour pairs (i.e. silica gel/water), which are considered more suitable for integration with PEMFC stacks, can improve the overall CCP/CCHP efficiency up to 60–65%. Absorptions chillers using liquid–vapour pairs (i.e. LiBr/water and water/ammonia) could be able to generate cooling capacities in the range of 50–90% with combined CCP/CCHP efficiency up to ~85%.

The efficiency of heat engines such as ORC, TEG, and TREC is limited by Carnot cycle efficiency; hence, waste heat recovery from PEMFC stacks for power cogeneration offers lower efficiencies in comparison with those offered by CHP and CCHP applications. However, from an engineering point of view, the combination of PEMFC stacks with ORC, TEG, and TREC technologies is technically feasible. At the same temperature heat sources, it seems that PEMFC heat recovery for TREC application offers better overall electrical efficiency than others (i.e. ORC and TEG). With the benefits of high operating temperature (120–200 °C), the waste heat recovery from HT-PEMFCs could be more favourable for power cogeneration applications compared to the LT-PEMFCs. Recent studies have indicated that capturing waste heat from PEMFCs for power cogeneration helps increase the overall efficiency of such hybrid systems (i.e. hybrid with ORC or TEG) by 3–5% and 5–9% for LT and HT-PEMFC systems, respectively. This improvement would be more attractive if they can be achieved at low costs while offering high durability.

In some applications, in which MH canisters are used for hydrogen storage, thermal management is necessary for matching the hydrogen release rate capacity by MH tanks with the hydrogen rate required by the PEM fuel cell stack (i.e. specially at higher power operating points). Thermal coupling of MH hydrogen storage with PEMFCs (capturing heat from the fuel cell stack to maintain the MH canisters' temperature and hydrogen release rate) offers a solution to this challenge and help enhance the performance of the whole system. MH tanks can be thermally-coupled with PEMFC stacks with different cooling strategies (passive and active). Usually, around 20–30% of the total heat generated by the fuel cell stack is enough to help increase the hydrogen release rate of the MH canisters to a desirable level.

The heat can be also captured and used for preheating cold inlet air and hydrogen reactants to the PEMFC stack itself in extreme cold climate environments (e.g. sub-zero ambient temperature). In such conditions, preheating the inlet air to above 0 °C is a technically-vital measure to prevent the stack from experiencing performance degradation and formation of ice in the membrane (especially during the start-up phase). Furthermore, increasing the temperature of inlet reactants (i.e. air and hydrogen) increases the open circuit voltage and decreases the activation losses; hence, the performance of the PEMFC stacks is improved.

While heat recovery opportunities from PEMFCs has been widely studies to date, less attention has been paid to the economic assessment of such systems, leaving this important matter to be a gap in the literature. Conducting thorough exergy analyses on such systems helps shed light on understanding the techno-economic performance of fuel cell heat recovery solutions. In addition, considering the possibilities for more than one thermal applications (i.e. combining both CHP and thermal management of MH systems) can potentially increase the performance of a PEMFC heat recovery solution. Finally, capturing the fuel cell heat for desalination and fresh water production needs further investigation.

Declaration of Competing Interest

The authors declare that they have no known competing financial interests or personal relationships that could have appeared to influence the work reported in this paper.

Acknowledgements

The authors express their sincere thanks to Australian Department of Education for an Endeavour Postgraduate Leadership Award to Huy Quoc Nguyen to pursue his PhD study at RMIT University, Australia. The supports from Danang University of Science and Technology (DUT), Vietnam, to follow up this PhD program by Huy Quoc Nguyen is also acknowledged.

References

[1] Andrews J, Shabani B. Re-envisioning the role of hydrogen in a sustainable energy economy. Int J Hydrogen Energy 2012;37:1184–203.
[2] Andrews J, Shabani B. Where does hydrogen fit in a sustainable energy economy? Proc Eng 2012;49:15–25.
[3] Shabani B, Andrews J. Hydrogen and fuel cells. Energy sustainability through green energy. Springer; 2015. p. 453–91.
[4] Gray EM, Webb C, Andrews J, Shabani B, Tsai P, Chan S. Hydrogen storage for off-grid power supply. Int J Hydrogen Energy 2011;36:654–63.
[5] Shabani B, Andrews J. Standalone solar-hydrogen systems powering fire contingency networks. Int J Hydrogen Energy 2015;40:5509–17.
[6] Yilanci A, Dincer I, Ozturk H. A review on solar-hydrogen/fuel cell hybrid energy systems for stationary applications. Prog Energy Combust Sci 2009;35:231–44.
[7] Maniatopoulos P, Andrews J, Shabani B. Towards a sustainable strategy for road transportation in Australia: the potential contribution of hydrogen. Renewable Sustainable Energy Rev 2015;52:24–34.
[8] Kharel S, Shabani B. Hydrogen as a long-term large-scale energy storage solution to support renewables. Energies 2018;11:2825.
[9] Brandon N, Kurban Z. Clean energy and the hydrogen economy. Phil Trans R Soc A 2017;375:20160400.
[10] Andrews J, Shabani B. The role of hydrogen in a global sustainable energy strategy. Wiley Interdiscip. Rev.: Energy Environ. 2014;3:474–89.
[11] Elmer T, Worall M, Wu S, Riffat SB. Fuel cell technology for domestic built environment applications: state of-the-art review. Renewable Sustainable Energy Rev 2015;42:913–31.
[12] Ellamla HR, Staffell I, Bujlo P, Pollet BG, Pasupathi S. Current status of fuel cell based combined heat and power systems for residential sector. J Power Sources 2015;293:312–28.
[13] Onovwiona HI, Ugursal VI. Residential cogeneration systems: review of the current technology. Renewable Sustainable Energy Rev 2006;10:389–431.
[14] Shabani B. Solar-hydrogen combined heat and power systems for remote area power supply. RMIT University; 2010.
[15] Dicks AL, Rand DA. Fuel cell systems explained. John Wiley & Sons; 2018.
[16] Zhang G, Kandlikar SG. A critical review of cooling techniques in proton exchange membrane fuel cell stacks. Int J Hydrogen Energy 2012;37:2412–29.
[17] Hossain MS, Shabani B. Metal foams application to enhance cooling of open cathode polymer electrolyte membrane fuel cells. J Power Sources 2015;295:275–91.
[18] Chen X, Chen L, Guo J, Chen J. An available method exploiting the waste heat in a proton exchange membrane fuel cell system. Int J Hydrogen Energy 2011;36:6099–104.
[19] Zhao P, Wang J, Gao L, Dai Y. Parametric analysis of a hybrid power system using organic Rankine cycle to recover waste heat from proton exchange membrane fuel cell. Int J Hydrogen Energy 2012;37:3382–91.
[20] Nguyen G, Sahlin S, Andreasen SJ, Shaffer B, Brouwer J. Dynamic modeling and experimental investigation of a high temperature PEM fuel cell stack. Int J Hydrogen Energy 2016;41:4729–39.
[21] Rosli R, Sulong A, Daud W, Zulkifley M, Husaini T, Rosli M, et al. A review of high-temperature proton exchange membrane fuel cell (HT-PEMFC) system. Int J Hydrogen Energy 2017;42:9293–314.
[22] Shabani B, Andrews J, Badwal S. Fuel cell heat recovery, electrical load management, and the economics of solar-hydrogen systems. Int J Power Energy Syst 2010;30:256.
[23] Faghri A, Guo Z. Challenges and opportunities of thermal management issues related to fuel cell technology and modeling. Int J Heat Mass Transf 2005;48:3891–920.
[24] Nguyen HQ, Aris AM, Shabani B. PEM fuel cell heat recovery for preheating inlet air in standalone solar-hydrogen systems for telecommunication applications: an exergy analysis. Int J Hydrogen Energy 2016;41:2987–3003.
[25] Islam MR, Shabani B, Rosengarten G. Nanofluids to improve the performance of PEM fuel cell cooling systems: a theoretical approach. Appl Energy 2016;178:660–71.
[26] Islam M, Shabani B, Rosengarten G, Andrews J. The potential of using nanofluids in PEM fuel cell cooling systems: a review. Renewable Sustainable Energy Rev 2015;48:523–39.
[27] Wang Y, Chen KS. PEM fuel cells: thermal and water management fundamentals. Momentum Press; 2013.
[28] Omrani R, Shabani B. Gas diffusion layer modifications and treatments for improving the performance of proton exchange membrane fuel cells and electrolysers: a review. Int J Hydrogen Energy 2017.
[29] Li H, Tang Y, Wang Z, Shi Z, Wu S, Song D, et al. A review of water flooding issues in the proton exchange membrane fuel cell. J Power Sources 2008;178:103–17.

[30] Hwang JJ, Zou ML, Chang WR, Su A, Weng FB, Wu W. Implementation of a heat recovery unit in a proton exchange membrane fuel cell system. Int J Hydrogen Energy 2010;35:8644–53.
[31] Briguglio N, Ferraro M, Brunaccini G, Antonucci V. Evaluation of a low temperature fuel cell system for residential CHP. Int J Hydrogen Energy 2011;36:8023–9.
[32] Gigliucci G, Petruzzi L, Cerelli E, Garzisi A, La Mendola A. Demonstration of a residential CHP system based on PEM fuel cells. J Power Sources 2004;131:62–8.
[33] Shabani B, Andrews J. An experimental investigation of a PEM fuel cell to supply both heat and power in a solar-hydrogen RAPS system. Int J Hydrogen Energy 2011;36:5442–52.
[34] Oh S-D, Kim K-Y, Oh S-B, Kwak H-Y. Optimal operation of a 1-kW PEMFC-based CHP system for residential applications. Appl Energy 2012;95:93–101.
[35] Gandiglio M, Lanzini A, Santarelli M, Leone P. Design and optimization of a proton exchange membrane fuel cell CHP system for residential use. Energy Build 2014;69:381–93.
[36] Barelli L, Bidini G, Gallorini F, Ottaviano A. An energetic–exergetic comparison between PEMFC and SOFC-based micro-CHP systems. Int J Hydrogen Energy 2011;36:3206–14.
[37] Aleknaviciute I, Karayiannis T, Collins M, Xanthos C. Towards clean and sustainable distributed energy system: the potential of integrated PEMFC-CHP. Int J Low Carbon Technol 2016;11:296–304.
[38] Oh ST, Saha BB, Kariya K, Hamamoto Y, Mori H. Fuel cell waste heat powered adsorption cooling systems. Int J Air Conditioning Refrig 2013;21:1350010.
[39] He T, Shi R, Peng J, Zhuge W, Zhang Y. Waste heat recovery of a PEMFC system by using organic rankine cycle. Energies 2016;9:267.
[40] Lee W-Y, Kim M, Sohn Y-J, Kim S-G. Power optimization of a combined power system consisting of a high-temperature polymer electrolyte fuel cell and an organic Rankine cycle system. Energy 2016;113:1062–70.
[41] Hasani M, Rahbar N. Application of thermoelectric cooler as a power generator in waste heat recovery from a PEM fuel cell–an experimental study. Int J Hydrogen Energy 2015;40:15040–51.
[42] Tetuko AP, Shabani B, Andrews J. Thermal coupling of PEM fuel cell and metal hydride hydrogen storage using heat pipes. Int J Hydrogen Energy 2016;41:4264–77.
[43] Tetuko AP, Shabani B, Andrews J. Passive fuel cell heat recovery using heat pipes to enhance metal hydride canisters hydrogen discharge rate: an experimental simulation. Energies 2018;11:915.
[44] Reddy EH, Jayanti S. Thermal coupling studies of a high temperature proton exchange membrane fuel cell stack and a metal hydride hydrogen storage system. Energy Proc 2012;29:254–64.
[45] Mohamed WANW, Kamil MHM. Hydrogen preheating through waste heat recovery of an open-cathode PEM fuel cell leading to power output improvement. Energy Convers Manage 2016;124:543–55.
[46] Ganapathy V. Industrial boilers and heat recovery steam generators; 2003.
[47] Tchanche BF, Lambrinos G, Frangoudakis A, Papadakis G. Low-grade heat conversion into power using organic Rankine cycles–a review of various applications. Renewable Sustainable Energy Rev 2011;15:3963–79.
[48] Stijepovic MZ, Linke P. Optimal waste heat recovery and reuse in industrial zones. Energy 2011;36:4019–31.
[49] Assaf J, Shabani B. A novel hybrid renewable solar energy solution for continuous heat and power supply to standalone-alone applications with ultimate reliability and cost effectiveness. Renewable Energy 2019;138:509–20.
[50] Milcarek RJ, Ahn J, Zhang J. Review and analysis of fuel cell-based, micro-cogeneration for residential applications: Current state and future opportunities. Sci Technol Built Environ 2017;23:1224–43.
[51] Özgür T, Yakaryılmaz AC. A review: exergy analysis of PEM and PEM fuel cell based CHP systems. Int J Hydrogen Energy 2018.
[52] Bvumbe TJ, Bujlo P, Tolj I, Mouton K, Swart G, Pasupathi S, et al. Review on management, mechanisms and modelling of thermal processes in PEMFC. Hydrogen Fuel Cells 2016;1:1–20.
[53] Kandlikar SG, Lu Z. Thermal management issues in a PEMFC stack–a brief review of current status. Appl Therm Eng 2009;29:1276–80.
[54] Ramousse J, Lottin O, Didierjean S, Maillet D. Heat sources in proton exchange membrane (PEM) fuel cells. J Power Sources 2009;192:435–41.
[55] Graf C, Vath A, Nicoloso N. Modeling of the heat transfer in a portable PEFC system within MATLAB-Simulink. J Power Sources 2006;155:52–9.
[56] Zhang G, Yuan H, Wang Y, Jiao K. Three-dimensional simulation of a new cooling strategy for proton exchange membrane fuel cell stack using a non-isothermal multiphase model. Appl Energy 2019;255. 113865.
[57] Wang Y, Ruiz Diaz DF, Chen KS, Wang Z, Adroher XC. Materials, technological status, and fundamentals of PEM fuel cells – a review. Mater Today 2019.
[58] Wen C-Y, Lin Y-S, Lu C-H. Performance of a proton exchange membrane fuel cell stack with thermally conductive pyrolytic graphite sheets for thermal management. J Power Sources 2009;189:1100–5.
[59] Burke KA, Jakupca IJ, Colozza AJ. Development of passive fuel cell thermal. Manage Heat Exch 2010.
[60] Wen C-Y, Lin Y-S, Lu C-H, Luo T-W. Thermal management of a proton exchange membrane fuel cell stack with pyrolytic graphite sheets and fans combined. Int J Hydrogen Energy 2011;36:6082–9.
[61] Jang J-Y, Tsai Y-C. Optimization of thermoelectric generator module spacing and spreader thickness used in a waste heat recovery system. Appl Therm Eng 2013;51:677–89.
[62] Remeli MF, Tan L, Date A, Singh B, Akbarzadeh A. Simultaneous power generation and heat recovery using a heat pipe assisted thermoelectric generator system. Energy Convers Manage 2015;91:110–9.
[63] Supra J, Janßen H, Lehnert W, Stolten D. Design and experimental investigation of a heat pipe supported external cooling system for HT-PEFC stacks. J Fuel Cell Sci Technol 2013;10. 051002.
[64] Legierski J, Wie B, De Mey G. Measurements and simulations of transient characteristics of heat pipes. Microelectron Reliab 2006;46:109–15.
[65] Solomon AB, Sekar M, Yang SH. Analytical expression for thermal conductivity of heat pipe. Appl Therm Eng 2016;100:462–7.
[66] Burke K, Jakupca I, Colozza A. Development of passive fuel cell thermal management technology. In: 7th International Energy Conversion Engineering Conference; 2010. p. 4656.
[67] Tetuko AP, Shabani B, Omrani R, Paul B, Andrews J. Study of a thermal bridging approach using heat pipes for simultaneous fuel cell cooling and metal hydride hydrogen discharge rate enhancement. J Power Sources 2018;397:177–88.
[68] Oro MV, Bazzo E. Flat heat pipes for potential application in fuel cell cooling. Appl Therm Eng 2015;90:848–57.
[69] Clement J, Wang X. Experimental investigation of pulsating heat pipe performance with regard to fuel cell cooling application. Appl Therm Eng 2013;50:268–74.
[70] Vasiliev LL. Heat pipes in modern heat exchangers. Appl Therm Eng 2005;25:1–19.
[71] Vasiliev L. Heat pipes in fuel cell technology. Mini-micro fuel cells. Springer; 2008. p. 117–24.
[72] Andreasen SrJ, Kær SrK. 400 W high temperature PEM fuel cell stack test. Ecs Transactions. vol. 5; 2007. p. 197–207.
[73] Shahsavari S, Desouza A, Bahrami M, Kjeang E. Thermal analysis of air-cooled PEM fuel cells. Int J Hydrogen Energy 2012;37:18261–71.
[74] Sasmito A, Lum K, Birgersson E, Mujumdar A. Computational study of forced air-convection in open-cathode polymer electrolyte fuel cell stacks. J Power Sources 2010;195:5550–63.
[75] Sohn Y-J, Park G-G, Yang T-H, Yoon Y-G, Lee W-Y, Yim S-D, et al. Operating characteristics of an air-cooling PEMFC for portable applications. J Power Sources 2005;145:604–9.
[76] Shah A, Luo K, Ralph T, Walsh F. Recent trends and developments in polymer electrolyte membrane fuel cell modelling. Electrochim Acta 2011;56:3731–57.
[77] Matian M, Marquis A, Brandon N. Model based design and test of cooling plates for an air-cooled polymer electrolyte fuel cell stack. Int J Hydrogen Energy 2011;36:6051–66.
[78] Ballard. Fuel Cell Stacks.
[79] HorizonFuelCell. H-Series 10W-5kW PEM Stack Modules.
[80] PowerCell. PowerCell Fuel Cell Stacks. PowerCell; 2019.
[81] PowerCell. PowerCell Fuel Cell Stacks. PowerCell; 2019.
[82] Sasmito AP, Birgersson E, Mujumdar AS. Numerical evaluation of various thermal management strategies for polymer electrolyte fuel cell stacks. Int J Hydrogen Energy 2011;36:12991–3007.
[83] Soupremanien U, Le Person S, Favre-Marinet M, Bultel Y. Tools for designing the cooling system of a proton exchange membrane fuel cell. Appl Therm Eng 2012;40:161–73.
[84] Kang K, Yoo H, Han D, Jo A, Lee J, Ju H. Modeling and simulations of fuel cell systems for combined heat and power generation. Int J Hydrogen Energy 2016;41:8286–95.
[85] Jo A, Oh K, Lee J, Han D, Kim D, Kim J, et al. Modeling and analysis of a 5 kWe HT-PEMFC system for residential heat and power generation. Int J Hydrogen Energy 2017;42:1698–714.
[86] Chen X, Zhou H, Li W, Yu Z, Gong G, Yan Y, et al. Multi-criteria assessment and optimization study on 5 kW PEMFC based residential CCHP system. Energy Convers Manage 2018;160:384–95.
[87] Perna A, Minutillo M, Jannelli E. Investigations on an advanced power system based on a high temperature polymer electrolyte membrane fuel cell and an organic Rankine cycle for heating and power production. Energy 2015;88:874–84.
[88] Oro MV, de Oliveira RG, Bazzo E. An integrated solution for waste heat recovery from fuel cells applied to adsorption systems. Appl Therm Eng 2018;136:747–54.
[89] Chen X, Gong G, Wan Z, Luo L, Wan J. Performance analysis of 5 kW PEMFC-based residential micro-CCHP with absorption chiller. Int J Hydrogen Energy 2015;40:10647–57.
[90] Deng W, Dai C, Guo A, Chen W. Waste heat utilization in fuel cell trams with thermoelectric generators. Chinese Automation Congress (CAC), 2017. IEEE2017. p. 1992–1997.
[91] Zakaria I, Azmi WH, Mohamed WANW, Mamat R, Najafi G. Experimental investigation of thermal conductivity and electrical conductivity of Al_2O_3 nanofluid in water - ethylene glycol mixture for proton exchange membrane fuel cell application. Int Commun Heat Mass Transfer 2015;61:61–8.
[92] Islam R, Shabani B, Andrews J, Rosengarten G. Experimental investigation of using ZnO nanofluids as coolants in a PEM fuel cell. Int J Hydrogen Energy 2017;42:19272–86.
[93] Islam MR, Shabani B, Rosengarten G. Electrical and thermal conductivities of 50/50 water-ethylene glycol based TiO2 nanofluids to be used as coolants in PEM fuel cells. Energy Proc 2017;110:101–8.
[94] Islam R, Shabani B. Prediction of electrical conductivity of TiO2 water and ethylene glycol-based nanofluids for cooling application in low temperature PEM fuel cells. Energy Proc 2019;160:550–7.
[95] Perry ML, Meyers JP, Darling RM, Evans C, Balliet R. Evaporatively-cooled pem fuel-cell stack and system. ECS Trans 2006;3:1207–14.
[96] Darling RM, Perry ML. Evaporatively cooled hybrid PEM fuel cell power plant assembly. Google Patents; 2011.
[97] Reiser CA, Meyers JP, Johnson JP, Evans CE, Darling RM, Skiba T, et al. Fuel cells evaporative reactant gas cooling and operational freeze prevention. Google Patents; 2009.
[98] Maisotsenko V, Gillan LE, Heaton TL, Gillan AD. Fuel cell systems with evaporative

cooling and methods for humidifying and adjusting the temperature of the reactant streams. Google Patents; 2004.
[99] Fly A, Thring RH. A comparison of evaporative and liquid cooling methods for fuel cell vehicles. Int J Hydrogen Energy 2016;41:14217–29.
[100] Brambilla M, Mazzucchelli G. Fuel cell with cooling system based on direct injection of liquid water. Google Patents; 2004.
[101] Goebel SG. Evaporative cooled fuel cell. Google Patents; 2005.
[102] Weber AZ, Darling RM. Understanding porous water-transport plates in polymer-electrolyte fuel cells. J Power Sources 2007;168:191–9.
[103] Garrity PT, Klausner JF, Mei R. A flow boiling microchannel evaporator plate for fuel cell thermal management. Heat Transfer Eng 2007;28:877–84.
[104] Song T-W, Choi K-H, Kim J-R, Jung SY. Pumpless thermal management of water-cooled high-temperature proton exchange membrane fuel cells. J Power Sources 2011;196:4671–9.
[105] Barbir F, Gomez T. Efficiency and economics of proton exchange membrane (PEM) fuel cells. Int J Hydrogen Energy 1997;22:1027–37.
[106] Hou Y, Wang B, Yang Z. A method for evaluating the efficiency of PEM fuel cell engine. Appl Energy 2011;88:1181–6.
[107] Brückner S, Liu S, Miró L, Radspieler M, Cabeza LF, Lävemann E. Industrial waste heat recovery technologies: an economic analysis of heat transformation technologies. Appl Energy 2015;151:157–67.
[108] Zhang X, Chan S, Li G, Ho H, Li J, Feng Z. A review of integration strategies for solid oxide fuel cells. J Power Sources 2010;195:685–702.
[109] Choudhury A, Chandra H, Arora A. Application of solid oxide fuel cell technology for power generation—a review. Renew Sustain Energy Rev 2013;20:430–42.
[110] Adam A, Fraga ES, Brett DJ. Options for residential building services design using fuel cell based micro-CHP and the potential for heat integration. Appl Energy 2015;138:685–94.
[111] Chen H, Goswami DY, Stefanakos EK. A review of thermodynamic cycles and working fluids for the conversion of low-grade heat. Renewable Sustainable Energy Rev 2010;14:3059–67.
[112] Sun J, Fu L, Zhang S. A review of working fluids of absorption cycles. Renewable Sustainable Energy Rev 2012;16:1899–906.
[113] Ebrahimi K, Jones GF, Fleischer AS. A review of data center cooling technology, operating conditions and the corresponding low-grade waste heat recovery opportunities. Renewable Sustainable Energy Rev 2014;31:622–38.
[114] Champier D. Thermoelectric generators: a review of applications. Energy Convers Manage 2017;140:167–81.
[115] Shabani B, Andrews J, Watkins S. Energy and cost analysis of a solar-hydrogen combined heat and power system for remote power supply using a computer simulation. Sol Energy 2010;84:144–55.
[116] Hwang J-J. Transient efficiency measurement of a combined heat and power fuel cell generator. J Power Sources 2013;223:325–35.
[117] Hwang JJ, Zou ML. Development of a proton exchange membrane fuel cell cogeneration system. J Power Sources 2010;195:2579–85.
[118] Hwang JJ, Wang PC, Kuo JK. Simulation and experiment of a cogeneration system based on proton exchange membrane fuel cell. Fuel Cells 2012;12:326–34.
[119] Saidi M, Ehyaei M, Abbasi A. Optimization of a combined heat and power PEFC by exergy analysis. J Power Sources 2005;143:179–84.
[120] Abdin Z, Webb C, Gray EM. Solar hydrogen hybrid energy systems for off-grid electricity supply: a critical review. Renewable Sustainable Energy Rev 2015;52:1791–808.
[121] Moore J, Shabani B. A critical study of stationary energy storage policies in Australia in an international context: the role of hydrogen and battery technologies. Energies 2016;9:674.
[122] Shabani B, Biju M. Theoretical modelling methods for thermal management of batteries. Energies 2015;8:10153–77.
[123] Zini G, Tartarini P. Hybrid systems for solar hydrogen: a selection of case-studies. Appl Therm Eng 2009;29:2585–95.
[124] Silva SB, Severino MM, de Oliveira MAG. A stand-alone hybrid photovoltaic, fuel cell and battery system: A case study of Tocantins, Brazil. Renewable Energy 2013;57:384–9.
[125] Giatrakos GP, Tsoutsos TD, Mouchtaropoulos PG, Naxakis GD, Stavrakakis G. Sustainable energy planning based on a stand-alone hybrid renewableenergy/hydrogen power system: Application in Karpathos island, Greece. Renewable Energy. 2009;34:2562–70.
[126] Ghribi D, Khelifa A, Diaf S, Belhamel M. Study of hydrogen production system by using PV solar energy and PEM electrolyser in Algeria. Int J Hydrogen Energy 2013;38:8480–90.
[127] Ural Z, Gencoglu MT. Design and simulation of a solar-hydrogen system for different situations. Int J Hydrogen Energy 2014;39:8833–40.
[128] Andrews J, Shabani B. Dimensionless analysis of the global techno-economic feasibility of solar-hydrogen systems for constant year-round power supply. Int J Hydrogen Energy 2012;37:6–18.
[129] Cetin E, Yilanci A, Oner Y, Colak M, Kasikci I, Ozturk HK. Electrical analysis of a hybrid photovoltaic-hydrogen/fuel cell energy system in Denizli, Turkey. Energy Build 2009;41:975–81.
[130] Khan MJ, Iqbal MT. Analysis of a small wind-hydrogen stand-alone hybrid energy system. Appl Energy 2009;86:2429–42.
[131] Carton JG, Olabi AG. Wind/hydrogen hybrid systems: Opportunity for Ireland's wind resource to provide consistent sustainable energy supply. Energy 2010;35:4536–44.
[132] Rahimi S, Meratizaman M, Monadizadeh S, Amidpour M. Techno-economic analysis of wind turbine–PEM (polymer electrolyte membrane) fuel cell hybrid system in standalone area. Energy 2014;67:381–96.
[133] Nelson D, Nehrir M, Wang C. Unit sizing and cost analysis of stand-alone hybrid wind/PV/fuel cell power generation systems. Renewable Energy 2006;31:1641–56.
[134] Eroglu M, Dursun E, Sevencan S, Song J, Yazici S, Kilic O. A mobile renewable house using PV/wind/fuel cell hybrid power system. Int J Hydrogen Energy 2011;36:7985–92.
[135] Sichilalu S, Tazvinga H, Xia X. Optimal control of a fuel cell/wind/PV/grid hybrid system with thermal heat pump load. Sol Energy 2016;135:59–69.
[136] Aris A, Shabani B. Sustainable power supply solutions for off-grid base stations. Energies 2015;8:10904–41.
[137] Barbir F. PEM electrolysis for production of hydrogen from renewable energy sources. Sol Energy 2005;78:661–9.
[138] Shabani B, Hafttananian M, Khamani S, Ramiar A, Ranjbar A. Poisoning of proton exchange membrane fuel cells by contaminants and impurities: review of mechanisms, effects, and mitigation strategies. J Power Sources 2019;427:21–48.
[139] Hafttananian M, Ramiar A, Shabani B, Ranjbar A. Nonlinear algorithm of PEM fuel cell catalyst poisoning progress in the presence of carbon monoxide in anode fuel: a computational study using OpenFOAM. Electrochim Acta 2017;246:348–64.
[140] Ni M, Leung MKH, Leung DYC. Energy and exergy analysis of hydrogen production by a proton exchange membrane (PEM) electrolyzer plant. Energy Convers Manage 2008;49:2748–56.
[141] Ursua A, Gandia LM, Sanchis P. Hydrogen production from water electrolysis: current status and future trends. Proc IEEE 2012;100:410–26.
[142] Buttler A, Spliethoff H. Current status of water electrolysis for energy storage, grid balancing and sector coupling via power-to-gas and power-to-liquids: a review. Renewable Sustainable Energy Rev 2018;82:2440–54.
[143] Lacko R, Drobnič B, Mori M, Sekavčnik M, Vidmar M. Stand-alone renewable combined heat and power system with hydrogen technologies for household application. Energy 2014;77:164–70.
[144] Pedrazzi S, Zini G, Tartarini P. Modelling and simulation of a wind-hydrogen CHP system with metal hydride storage. Renewable Energy 2012;46:14–22.
[145] Zafar S, Dincer I. Thermodynamic analysis of a combined PV/T–fuel cell system for power, heat, fresh water and hydrogen production. Int J Hydrogen Energy 2014;39:9962–72.
[146] Nowotny J, Sorrell C, Sheppard L, Bak T. Solar-hydrogen: environmentally safe fuel for the future. Int J Hydrogen Energy 2005;30:521–44.
[147] Ito H, Miyazaki N, Ishida M, Nakano A. Efficiency of unitized reversible fuel cell systems. Int J Hydrogen Energy 2016;41:5803–15.
[148] Isa NM, Das HS, Tan CW, Yatim A, Lau KY. A techno-economic assessment of a combined heat and power photovoltaic/fuel cell/battery energy system in Malaysia hospital. Energy 2016;112:75–90.
[149] Maleki A, Khajeh MG, Rosen MA. Two heuristic approaches for the optimization of grid-connected hybrid solar–hydrogen systems to supply residential thermal and electrical loads. Sustainable Cities Soc 2017;34:278–92.
[150] Lagorse J, Simões MG, Miraoui A, Costerg P. Energy cost analysis of a solar-hydrogen hybrid energy system for stand-alone applications. Int J Hydrogen Energy 2008;33:2871–9.
[151] Assaf J, Shabani B. Multi-objective sizing optimisation of a solar-thermal system integrated with a solar-hydrogen combined heat and power system, using genetic algorithm. Energy Convers Manage 2018;164:518–32.
[152] Assaf J, Shabani B. Transient simulation modelling and energy performance of a standalone solar-hydrogen combined heat and power system integrated with solar-thermal collectors. Appl Energy 2016;178:66–77.
[153] Napoli R, Gandiglio M, Lanzini A, Santarelli M. Techno-economic analysis of PEMFC and SOFC micro-CHP fuel cell systems for the residential sector. Energy Build 2015;103:131–46.
[154] Vadiee A, Yaghoubi M, Sardella M, Farjam P. Energy analysis of fuel cell system for commercial greenhouse application–a feasibility study. Energy Convers Manage 2015;89:925–32.
[155] Aki H, Wakui T, Yokoyama R. Development of an energy management system for optimal operation of fuel cell based residential energy systems. Int J Hydrogen Energy 2016;41:20314–25.
[156] Bianchi M, De Pascale A, Melino F. Performance analysis of an integrated CHP system with thermal and Electric Energy Storage for residential application. Appl Energy 2013;112:928–38.
[157] Vijay A, Hawkes A. Impact of dynamic aspects on economics of fuel cell based micro co-generation in low carbon futures. Energy 2018;155:874–86.
[158] Assaf J, Shabani B. Economic analysis and assessment of a standalone solar-hydrogen combined heat and power system integrated with solar-thermal collectors. Int J Hydrogen Energy 2016;41:18389–404.
[159] Assaf J, Shabani B. Experimental study of a novel hybrid solar-thermal/PV-hydrogen system: towards 100% renewable heat and power supply to standalone applications. Energy 2018;157:862–76.
[160] Choudhury B, Saha BB, Chatterjee PK, Sarkar JP. An overview of developments in adsorption refrigeration systems towards a sustainable way of cooling. Appl Energy 2013;104:554–67.
[161] Clausse M, Meunier F, Coulié J, Herail E. Comparison of adsorption systems using natural gas fired fuel cell as heat source, for residential air conditioning. Int J Refrig 2009;32:712–9.
[162] Pang S, Masjuki H, Kalam M, Hazrat M. Liquid absorption and solid adsorption system for household, industrial and automobile applications: a review. Renewable Sustainable Energy Rev 2013;28:836–47.
[163] Zhang X, Chen X, Lin B, Chen J. Maximum equivalent efficiency and power output of a PEM fuel cell/refrigeration cycle hybrid system. Int J Hydrogen Energy 2011;36:2190–6.
[164] Arsalis A. Modeling and simulation of a 100 kWe HT-PEMFC subsystem integrated with an absorption chiller subsystem. Int J Hydrogen Energy 2012;37:13484–90.

[165] Deng J, Wang R, Han G. A review of thermally activated cooling technologies for combined cooling, heating and power systems. Prog Energy Combust Sci 2011;37:172–203.
[166] Wang RZ, Xu ZY, Pan QW, Du S, Xia ZZ. Solar driven air conditioning and refrigeration systems corresponding to various heating source temperatures. Appl Energy 2016;169:846–56.
[167] Saha BB, Koyama S, Kashiwagi T, Akisawa A, Ng KC, Chua HT. Waste heat driven dual-mode, multi-stage, multi-bed regenerative adsorption system. Int J Refrig 2003;26:749–57.
[168] Wang L, Wang R, Oliveira R. A review on adsorption working pairs for refrigeration. Renewable Sustainable Energy Rev 2009;13:518–34.
[169] Pilatowsky I, Romero R, Isaza C, Gamboa S, Rivera W, Sebastian P, et al. Simulation of an air conditioning absorption refrigeration system in a co-generation process combining a proton exchange membrane fuel cell. Int J Hydrogen Energy 2007;32:3174–82.
[170] Cozzolino R. Thermodynamic performance assessment of a novel micro-CCHP system based on a low temperature PEMFC power unit and a half-effect Li/Br absorption chiller. Energies 2018;11:315.
[171] Chahartaghi M, Kharkeshi BA. Performance analysis of a combined cooling, heating and power system with PEM fuel cell as a prime mover. Appl Therm Eng 2018;128:805–17.
[172] Chen X, Gong G, Wan Z, Zhang C, Tu Z. Performance study of a dual power source residential CCHP system based on PEMFC and PTSC. Energy Convers Manage 2016;119:163–76.
[173] Yang P, Zhang H. Parametric analysis of an irreversible proton exchange membrane fuel cell/absorption refrigerator hybrid system. Energy 2015;85:458–67.
[174] Sadeghi S, Maghsoudi P, Shabani B, Gorgani HH, Shabani N. Performance analysis and multi-objective optimization of an organic Rankine cycle with binary zeotropic working fluid employing modified artificial bee colony algorithm. J Therm Anal Calorim 2019;136:1645–65.
[175] Hung TC, Shai TY, Wang SK. A review of organic rankine cycles (ORCs) for the recovery of low-grade waste heat. Energy 1997;22:661–7.
[176] Tchanche BF, Lambrinos G, Frangoudakis A, Papadakis G. Low-grade heat conversion into power using organic Rankine cycles – a review of various applications. Renewable Sustainable Energy Rev 2011;15:3963–79.
[177] Bao J, Zhao L. A review of working fluid and expander selections for organic Rankine cycle. Renewable Sustainable Energy Rev 2013;24:325–42.
[178] Vélez F, Segovia JJ, Martín MC, Antolín G, Chejne F, Quijano A. A technical, economical and market review of organic Rankine cycles for the conversion of low-grade heat for power generation. Renewable Sustainable Energy Rev 2012;16:4175–89.
[179] Alijanpour Sheshpoli M, Mousavi Ajarostaghi SS. Delavar MA. Waste heat recovery from a 1180 kW proton exchange membrane fuel cell (PEMFC) system by Recuperative organic Rankine cycle (RORC). Energy 2018;157:353–66.
[180] Sheshpoli MA, Ajarostaghi SSM, Delavar MA. Thermodynamic analysis of waste heat recovery from hybrid system of proton exchange membrane fuel cell and vapor compression refrigeration cycle by recuperative organic Rankine cycle. J Therm Anal Calorim 2019;135:1699–712.
[181] Lee JY, Lee JH, Kim TS. Thermo-economic analysis of using an organic Rankine cycle for heat recovery from both the cell stack and reformer in a PEMFC for power generation. Int J Hydrogen Energy 2019;44:3876–90.
[182] Orr B, Akbarzadeh A, Mochizuki M, Singh R. A review of car waste heat recovery systems utilising thermoelectric generators and heat pipes. Appl Therm Eng 2016;101:490–5.
[183] He W, Zhang G, Zhang X, Ji J, Li G, Zhao X. Recent development and application of thermoelectric generator and cooler. Appl Energy 2015;143:1–25.
[184] Crane DT, Jackson GS. Optimization of cross flow heat exchangers for thermoelectric waste heat recovery. Energy Convers Manage 2004;45:1565–82.
[185] Martín-González M, Caballero-Calero O, Díaz-Chao P. Nanoengineering thermoelectrics for 21st century: Energy harvesting and other trends in the field. Renewable Sustainable Energy Rev 2013;24:288–305.
[186] Gao X, Andreasen SJ, Kær SK, Rosendahl LA. Optimization of a thermoelectric generator subsystem for high temperature PEM fuel cell exhaust heat recovery. Int J Hydrogen Energy 2014;39:6637–45.
[187] Kwan TH, Wu X, Yao Q. Multi-objective genetic optimization of the thermoelectric system for thermal management of proton exchange membrane fuel cells. Appl Energy 2018;217:314–27.
[188] Kuo JK, Hwang JJ, Lin CH. Performance analysis of a stationary fuel cell thermoelectric cogeneration system. Fuel Cells 2012;12:1104–14.
[189] Gao X, Chen M, Andreasen SJ, Kær SK. Potential usage of thermoelectric devices in a high-temperature polymer electrolyte membrane (PEM) fuel cell system: two case studies. J Electron Mater 2012;41:1838–44.
[190] Chen M, Andreasen SJ, Rosendahl L, Kær SK, Condra T. System modeling and validation of a thermoelectric fluidic power source: proton exchange membrane fuel cell and thermoelectric generator (PEMFC-TEG). J Electron Mater 2010;39:1593–600.
[191] Bubnova O, Crispin X. Towards polymer-based organic thermoelectric generators. Energy Environ Sci 2012;5:9345–62.
[192] Singh DV, Pedersen E. A review of waste heat recovery technologies for maritime applications. Energy Convers Manage 2016;111:315–28.
[193] Du Y, Xu J, Paul B, Eklund P. Flexible thermoelectric materials and devices. Appl Mater Today 2018;12:366–88.
[194] Sulaiman MS, Mohamed W, Singh B, Ghazali MF. Validation of a Waste Heat Recovery Model for a 1kW PEM Fuel Cell using Thermoelectric Generator. IOP Conference Series: Materials Science and Engineering. IOP Publishing; 2017. p. 012148.
[195] Sulaiman MS, Singh B, Mohamed W. Experimental and theoretical study of thermoelectric generator waste heat recovery model for an ultra-low temperature PEM fuel cell powered vehicle. Energy 2019;179:628–46.
[196] Lee SW, Yang Y, Lee H-W, Ghasemi H, Kraemer D, Chen G, et al. An electrochemical system for efficiently harvesting low-grade heat energy. Nat Commun 2014;5:3942.
[197] Gao X, Andreasen SJ, Chen M, Kær SK. Numerical model of a thermoelectric generator with compact plate-fin heat exchanger for high temperature PEM fuel cell exhaust heat recovery. Int J Hydrogen Energy 2012;37:8490–8.
[198] Yang Y, Loomis J, Ghasemi H, Lee SW, Wang YJ, Cui Y, et al. Membrane-free battery for harvesting low-grade thermal energy. Nano Lett 2014;14:6578–83.
[199] Fathabadi H. Replacing commercial thermoelectric generators with a novel electrochemical device in low-grade heat applications. Energy 2019;174:932–7.
[200] Guo J, Wang Y, Gonzalez-Ayala J, Roco J, Medina A, Hernández AC. Continuous power output criteria and optimum operation strategies of an upgraded thermally regenerative electrochemical cycles system. Energy Convers Manage 2019;180:654–64.
[201] Fathabadi H. Internal combustion engine vehicles: converting the waste heat of the engine into electric energy to be stored in the battery. IEEE Trans Veh Technol 2018;67:9241–8.
[202] Gao C, Yin Y, Zheng L, Liu Y, Sim S, He Y, et al. Engineering the electrochemical temperature coefficient for efficient low-grade heat harvesting. Adv Funct Mater 2018;28:1803129.
[203] Chum HL. Review of thermally regenerative electrochemical systems. Solar Energy Research Institute; 1981.
[204] Zhang X, Cai L, Liao T, Zhou Y, Zhao Y, Chen J. Exploiting the waste heat from an alkaline fuel cell via electrochemical cycles. Energy 2018;142:983–90.
[205] Açıkkalp E, Ahmadi MH. Parametric investigation of phosphoric acid fuel cell - thermally regenerative electro chemical hybrid system. J Cleaner Prod 2018;203:585–600.
[206] Yang Y, Lee SW, Ghasemi H, Loomis J, Li X, Kraemer D, et al. Charging-free electrochemical system for harvesting low-grade thermal energy. Proc Natl Acad Sci 2014;111:17011–6.
[207] Long R, Li B, Liu Z, Liu W. Multi-objective optimization of a continuous thermally regenerative electrochemical cycle for waste heat recovery. Energy 2015;93:1022–9.
[208] Zhang F, Liu J, Yang W, Logan BE. A thermally regenerative ammonia-based battery for efficient harvesting of low-grade thermal energy as electrical power. Energy Environ Sci 2015;8:343–9.
[209] Jiang J, Tian H, He X, Zeng Q, Niu Y, Zhou T, et al. A CoHCF system with enhanced energy conversion efficiency for low-grade heat harvesting. J Mater Chem A 2019.
[210] Long R, Li B, Liu Z, Liu W. A hybrid system using a regenerative electrochemical cycle to harvest waste heat from the proton exchange membrane fuel cell. Energy 2015;93:2079–86.
[211] Wang Y, Cai L, Peng W, Zhou Y, Chen J. Maximal continuous power output and parametric optimum design of an electrochemical system driven by low-grade heat. Energy Convers Manage 2017;138:156–61.
[212] Zhang X, Pan Y, Cai L, Zhao Y, Chen J. Using electrochemical cycles to efficiently exploit the waste heat from a proton exchange membrane fuel cell. Energy Convers Manage 2017;144:217–23.
[213] Lototskyy MV, Tolj I, Pickering L, Sita C, Barbir F, Yartys V. The use of metal hydrides in fuel cell applications. Prog Nat Sci: Mater Int 2017;27:3–20.
[214] Nasrallah SB, Jemni A. Heat and mass transfer models in metal-hydrogen reactor. Int J Hydrogen Energy 1997;22:67–76.
[215] MacDonald BD, Rowe AM. Impacts of external heat transfer enhancements on metal hydride storage tanks. Int J Hydrogen Energy 2006;31:1721–31.
[216] Wijayanta AT, Nakaso K, Aoki T, Kitazato Y, Fukai J. Effect of pressure, composition and temperature characteristics on thermal response and overall reaction rates in a metal hydride tank. Int J Hydrogen Energy 2011;36:3529–36.
[217] Mohammadshahi S, Gray EM, Webb C. A review of mathematical modelling of metal-hydride systems for hydrogen storage applications. Int J Hydrogen Energy 2016;41:3470–84.
[218] Omrani R, Nguyen HQ, Shabani B. Open-cathode PEMFC heat utilisation to enhance hydrogen supply rate of metal hydride canisters. Energy Proc 2019;160:542–9.
[219] Førde T, Eriksen J, Pettersen A, Vie P, Ulleberg Ø. Thermal integration of a metal hydride storage unit and a PEM fuel cell stack. Int J Hydrogen Energy 2009;34:6730–9.
[220] Borzenko V, Eronin A. The use of air as heating agent in hydrogen metal hydride storage coupled with PEM fuel cell. Int J Hydrogen Energy 2016;41:23120–4.
[221] Urbanczyk R, Peil S, Bathen D, Heßke C, Burfeind J, Hauschild K, et al. HT-PEM fuel cell system with integrated complex metal hydride storage tank. Fuel Cells 2011;11:911–20.
[222] MacDonald BD, Rowe AM. A thermally coupled metal hydride hydrogen storage and fuel cell system. J Power Sources 2006;161:346–55.
[223] Davids MW, Tolj I, Jao T-C, Lototskyy M, Pasupathi S, Sita C. Development of a portable polymer electrolyte membrane fuel cell system using metal hydride as the hydrogen storage medium. ECS Trans 2016;75:553–62.
[224] Han HS, Cho C, Kim SY, Hyun JM. Performance evaluation of a polymer electrolyte membrane fuel cell system for powering portable freezer. Appl Energy 2013;105:125–37.
[225] Song C, Klebanoff LE, Johnson TA, Chao BS, Socha AF, Oros JM, et al. Using metal hydride H_2 storage in mobile fuel cell equipment: design and predicted performance of a metal hydride fuel cell mobile light. Int J Hydrogen Energy 2014;39:14896–911.

[226] Hwang JJ, Chang WR. Characteristic study on fuel cell/battery hybrid power system on a light electric vehicle. J Power Sources 2012;207:111–9.
[227] Khaitan SK, Raju M. Discharge dynamics of coupled fuel cell and metal hydride hydrogen storage bed for small wind hybrid systems. Int J Hydrogen Energy 2012;37:2344–52.
[228] Rizzi P, Pinatel E, Luetto C, Florian P, Graizzaro A, Gagliano S, et al. Integration of a PEM fuel cell with a metal hydride tank for stationary applications. J Alloy Compd 2015;645:S338–42.
[229] Lototskyy MV, Tolj I, Davids MW, Klochko YV, Parsons A, Swanepoel D, et al. Metal hydride hydrogen storage and supply systems for electric forklift with low-temperature proton exchange membrane fuel cell power module. Int J Hydrogen Energy 2016;41:13831–42.
[230] Lototskyy MV, Tolj I, Parsons A, Smith F, Sita C, Linkov V. Performance of electric forklift with low-temperature polymer exchange membrane fuel cell power module and metal hydride hydrogen storage extension tank. J Power Sources 2016;316:239–50.
[231] Yiotis AG, Kainourgiakis ME, Charalambopoulou GC, Stubos AK. A generic physical model for a thermally integrated high-temperature PEM fuel cell and sodium alanate tank system. Int J Hydrogen Energy 2015;40:14551–61.
[232] Weiss-Ungethüm J, Bürger I, Schmidt N, Linder M, Kallo J. Experimental investigation of a liquid cooled high temperature proton exchange membrane (HT-PEM) fuel cell coupled to a sodium alanate tank. Int J Hydrogen Energy 2014;39:5931–41.
[233] Baricco M, Bang M, Fichtner M, Hauback B, Linder M, Luetto C, et al. SSH2S: Hydrogen storage in complex hydrides for an auxiliary power unit based on high temperature proton exchange membrane fuel cells. J Power Sources 2017;342:853–60.
[234] Pfeifer P, Wall C, Jensen O, Hahn H, Fichtner M. Thermal coupling of a high temperature PEM fuel cell with a complex hydride tank. Int J Hydrogen Energy 2009;34:3457–66.
[235] Sakintuna B, Lamari-Darkrim F, Hirscher M. Metal hydride materials for solid hydrogen storage: a review. Int J Hydrogen Energy 2007;32:1121–40.
[236] Afzal M, Mane R, Sharma P. Heat transfer techniques in metal hydride hydrogen storage: a review. Int J Hydrogen Energy 2017.
[237] Khayrullina A, Blinov D, Borzenko V. Air heated metal hydride energy storage system design and experiments for microgrid applications. Int J Hydrogen Energy 2019;44:19168–76.
[238] Khayrullina AG, Blinov D, Borzenko V. Novel kW scale hydrogen energy storage system utilizing fuel cell exhaust air for hydrogen desorption process from metal hydride reactor. Energy 2019;183:1244–52.
[239] Kim KJ, Montoya B, Razani A, Lee KH. Metal hydride compacts of improved thermal conductivity. Int J Hydrogen Energy 2001;26:609–13.
[240] Hahne E, Kallweit J. Thermal conductivity of metal hydride materials for storage of hydrogen: experimental investigation. Int J Hydrogen Energy 1998;23:107–14.
[241] Groll M. Reaction beds for dry sorption machines. Heat Recovery Syst CHP 1993;13:341–6.
[242] Ahluwalia R, Peng J-K, Hua T. Bounding material properties for automotive storage of hydrogen in metal hydrides for low-temperature fuel cells. Int J Hydrogen Energy 2014;39:14874–86.
[243] Omrani R, Shabani B. Review of gas diffusion layer for proton exchange membrane-based technologies with a focus on unitised regenerative fuel cells. Int J Hydrogen Energy 2019.
[244] Najafi B, Mamaghani AH, Rinaldi F, Casalegno A. Long-term performance analysis of an HT-PEM fuel cell based micro-CHP system: operational strategies. Appl Energy 2015;147:582–92.
[245] Sasmito AP, Shamim T, Mujumdar AS. Passive thermal management for PEM fuel cell stack under cold weather condition using phase change materials (PCM). Appl Therm Eng 2013;58:615–25.
[246] Kazim A. Exergy analysis of a PEM fuel cell at variable operating conditions. Energy Convers Manage 2004;45:1949–61.
[247] Kwan TH, Yao Q. Exergetic and temperature analysis of a fuel cell-thermoelectric device hybrid system for the combined heat and power application. Energy Convers Manage 2018;173:1–14.
[248] Ghaffour N, Bundschuh J, Mahmoudi H, Goosen MF. Renewable energy-driven desalination technologies: a comprehensive review on challenges and potential applications of integrated systems. Desalination 2015;356:94–114.
[249] Eltawil MA, Zhengming Z, Yuan L. A review of renewable energy technologies integrated with desalination systems. Renewable Sustainable Energy Rev 2009;13:2245–62.
[250] Lai X, Long R, Liu Z, Liu W. A hybrid system using direct contact membrane distillation for water production to harvest waste heat from the proton exchange membrane fuel cell. Energy 2018;147:578–86.